Development of liquid chromatography method for fast and quantitative analysis of amino acids and related compounds

（液体クロマトグラフィーを用いた
アミノ酸類化合物の高速定量法の開発）

宋　　彦廷

Contents

Chapter 1. Introduction

Background and objective

Integrative analysis of molecular changes in biological systems is an emerging approach in biological research. Instead of analysis of individual components, integrative analysis focuses on interactions between components, and how these interactions give rise to functions [1]. Metabolomics/metabonomics is an important technological platform for such research [2-4]. In an organism, metabolites play vital roles in all biological activities [5]. Analysis of metabolites in a biological sample could provide new insight into the physiological, developmental, and pathological status of a biological system [6]. For comprehensive analysis, a large number of samples need to be analyzed. This is very challenging work, and puts great demand and high requirements on analytical technologies.

Analysis of biological samples usually takes a long time, which greatly delays the progress of a study. Such delay becomes more significant in the clinical field, as analysis of metabolites could bring about not only a better understanding of disease mechanisms, but also be useful for the development of tools for disease diagnosis. Therefore, faster determination methods for compounds in biological samples are necessary.

Compounds in biological samples are also very complex. For example, it has been estimated that there are least 2,000–3,000 small molecules in the metabolome of higher organisms [7], which indicates that it is very difficult to conduct precise analysis of individual compounds without interference from others. Inaccurate determination could lead to misunderstandings of biological activities or mistakes in disease diagnosis. This problem is especially significant for some essential compounds with trace amounts. In most cases, they cannot be determined, which

results in the important biological information contained within these compounds being lost.

The development of fast quantitative analytical methods for compounds in biological samples has been attracting significant interests from researchers. With regard to the analytical method, the common strategy is for compounds to be separated before quantitative determination is performed. A variety of separation techniques have been developed for analysis of biological compounds, such as gas chromatography [8-10], capillary electrophoresis [11-13], and high-performance liquid chromatography [14-16]. Among these methods, high-performance liquid chromatography (HPLC) has been frequently utilized because there are no special equipment requirements, it has higher reliability and wide application.

A particle packed column is typically used in a HPLC system. When an analyte passes through the column the width of its band broadens. Column efficiency is a quantitative evaluation of the extent of band broadening. In the theoretical model of chromatography by Martin and Synge [17], the column is treated as though it consists of discrete sections at which the solute partitions between the stationary phase and mobile phase. Each section has a theoretical plate, theoretical plate number (N) and a theoretical plate height (H) which determines column efficiency. The relationship between N and H may be expressed as Equation (1):

$$N = L/H \qquad (1)$$

L is the length of the column. A column's efficiency improves with an increase of N or a decrease of H and vice versa.

There are many factors contributing to band broadening. The van Deemter equation expresses the factors contributing to column efficiency [18]. It is expressed as Equation (2):

$$H = A + B/u + Cu \qquad (2)$$

In this equation, A describes the effect of eddy diffusion which is caused by non-ideal packing and irregular size of particles in the column. A is the main factor responsible for total band broadening in a particle-packed column [19]. The contribution of multiple paths to the theoretical plate heights could be expressed as: $H_p = 2\lambda d_p$, where

d_p is the average diameter of the packing particles, and λ is the constant for the consistency of the packing. A small distribution of particle size and a more regular packing of particles will produce a smaller value of λ. Based on this equation, smaller values of H_p can be obtained by smaller diameters in packing particles and more homogenous packing of particles.

B describes the longitudinal diffusion in the mobile phase. Because the concentration in the center part of the band is greater, more analytes will diffuse towards the band's forward and rear edges. This term is closely related to column packing, the solute's diffusion coefficient in the mobile phase, and velocity of the mobile phase.

C represents the rate of mass transfer of the analyte between the stationary phase and mobile phase. It was found to be related to a solute's diffusion coefficient in the stationary phase, a column's diameter, velocity of the mobile phase, and thickness of the stationary phase.

Based on these fundamentals, researchers have been able to greatly improve the separation efficiency of the column, for example, by synthesis of smaller particles and more homogeneous packing of particles [20]. By applying such, much higher separation efficiency has been achieved. However, current separation efficiency still does not meet the requirement of fast quantitative determination of biological samples.

To resolve the problem, several types of new columns have been developed, such as the monolithic silica column, the sub-2 μm particle column, and the core-shell column. The monolithic silica column (Figure 1-1) is a single piece of porous cross-linked silica. Macropores, with a pore diameter of 1–10 μm, have low flow resistance, which ensures high-speed separation at a relatively low column backpressure. Mesopores, with a pore diameter of about 10–20 nm, provide efficient separation because of sufficient surface area [21]. Sub-2 μm fully porous particle columns for ultra-high-pressure liquid chromatography have been utilized widely for biological compounds analysis because analysis time can be shortened greatly at higher flow rates during the mobile phase. However, it is suggested in recent papers

that the core-shell particle column should provide higher separation efficiency than the sub-2 μm fully porous particle column [22, 23]. The core-shell particle column is packed with particles in which solid cores surround porous silica shells (Figure 1-2). This semi-porous silica column provides a shorter diffusion path for a solute to minimize peak broadening and allows high speed separation with lower operating pressure of the column. Extremely narrow distribution in particle size greatly reduces eddy diffusion, which is the main factor contributing to band broadening.

There were, however, limitations to separation efficiency even in the new types of conventional particle packed columns because of irregularity in fluid flow in the mobile zone [24, 25]. With the development of precise fabrication technology, this problem was resolved by Regnier *et al*., who developed a microfabricated electrically-driven pillar array column on silicon and quartz wafers (Figure 1-3) [26, 27]. This column has a perfectly ordered internal structure, and can eliminate the major sources of irregularity in the mobile phase zone [28]. Based on simulation results calculated using computational fluid dynamics, the use of a pillar array column could greatly improve separation efficiency compared with the best packed column and the best monolithic column (Figure 1-4) [19].

Desmet *et al*. has also contributed to the development of pressure-driven reversed-phase liquid chromatography separation in ordered nonporous pillar array columns [29-31]. Although they were able to achieve a reduced plate height of as low as 1, the maximum theoretical plate number *N* was 4,000–5,000 over a column length of 10 mm. It is hard to obtain a high theoretical plate number with a short column on a chip and, therefore, a folded long column has to be used. In our group's previous research, a pillar array column with a length of 110 mm was folded by low dispersion turns on a chip and a maximum *N* value of 8,000 was obtained [32].

In my thesis, fast quantitative liquid chromatography methods are developed for the analysis of amino acids. Amino acids are extremely important biological compounds. They are not only regulators of many biological activities, such as cell signaling, gene expression, and protein phosphorylation cascades, but also precursors for the synthesis of proteins, hormones, and other low-molecular weight nitrogenous

substances [33]. The concentrations of amino acids and related compounds could indicate the physiological status. Recently, changes in amino acid concentrations in biological fluids were reported to have close relationships with some diseases, such as inflammatory bowel disease [34], diabetes [35], and Huntington's disease [36]. Therefore, the development of fast quantitative methods for the determination of amino acids in biological samples would assist in the prediction, diagnosis, and understanding of diseases. Such methods, when developed, will be essential tools in clinical fields.

In Chapters 3 and 4, monolithic silica columns and core-shell columns are discussed in the analysis of amino acids—the methods being applied to biological samples.

In Chapter 5, the pillar array column is examined for fast analysis of branched-chain amino acids (valine, isoleucine, leucine), which participate in many physiological activities. The concentrations of branched-chain amino acids in sports drinks and mouse plasma samples are also determined.

Chapter 6 discusses the fabrication of a gradient elution system just before the pillar array column on the microchip. The developed gradient elution system is applied for the separation of 4-fluoro-7-nitro-2,1,3-benzoxadiazole (NBD-F)-aliphatic amines, which are involved in many biological reactions, such as the biodegradation of proteins, amino acids, and other biological compounds [37].

Figures

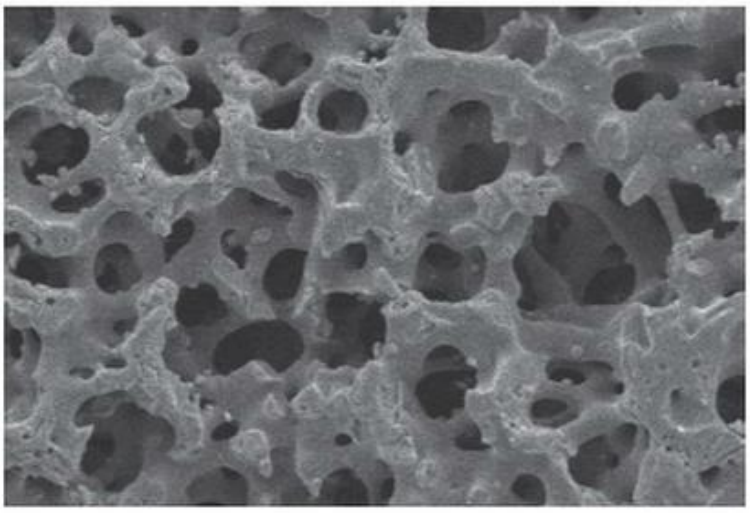

Figure 1-1. Internal structure of a monolithic silica column
(http://abh30.com/glsciences/general_catalog30/_SWF_Window.html)

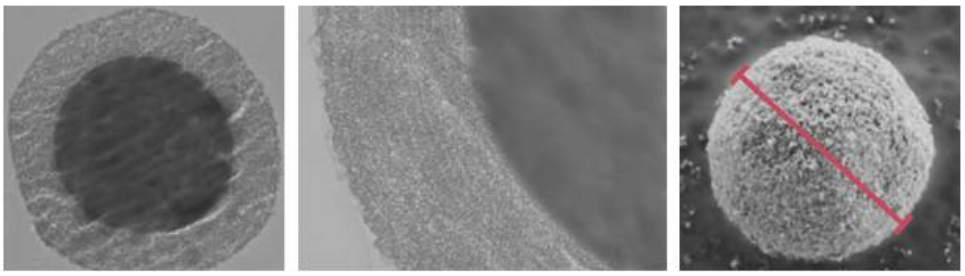

Figure 1-2. Transmission Electron Microscopy (TEM) and Scanning Electron Microscopy (SEM) images of a Kinetex core-shell particle column
(http://www.phenomenex.com/Aeris/AerisCoreShellStory?culture=ja)

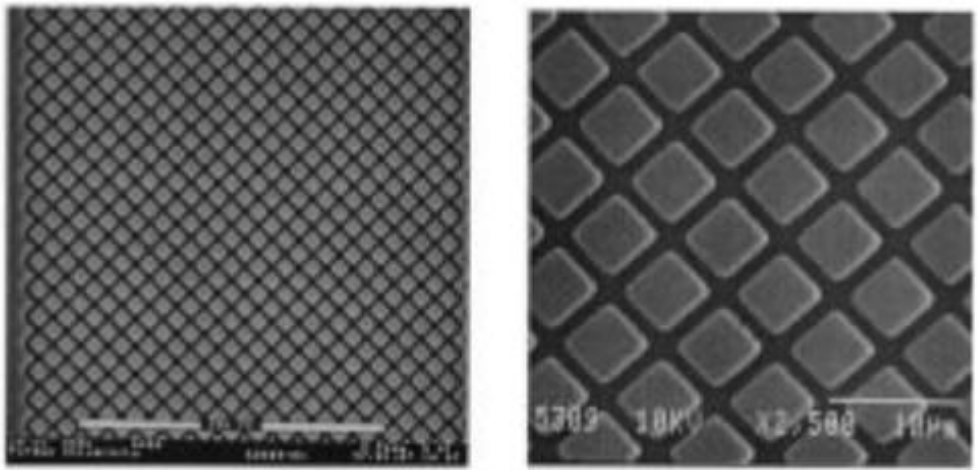

Figure 1-3. SEM images of microfabricated pillar array column

(B. He and F. Regnier, *Anal. Chem.*, 1998, 70, 3790-3797)

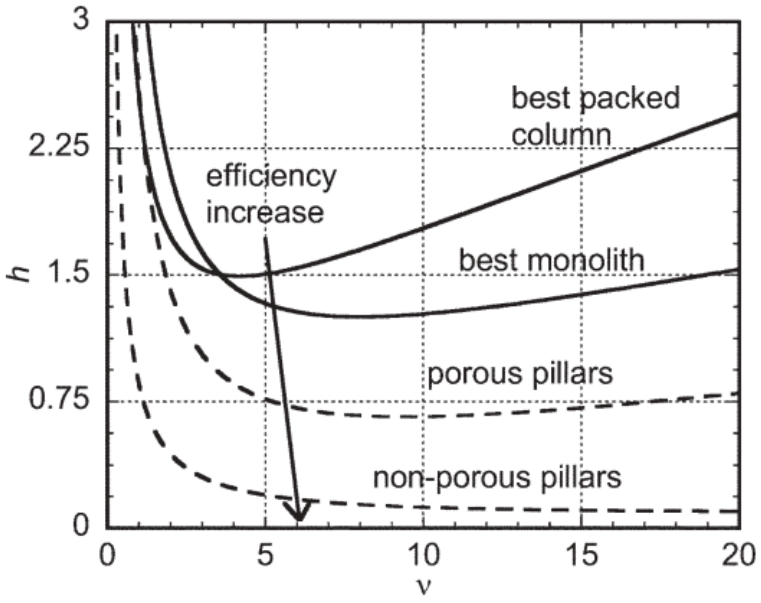

Figure 1-4. Reduced van Deemter's plot simulated by computational fluid dynamics

(J. Eijkel, *Lab Chip*, 2007, 7, 815-817)

Chapter 2. Materials and equipments

2.1 Reagents

Acetonitrile (HPLC grade)	Honeywell Burdick & Jackson (Muskegon, MI, USA)
Alanine (Ala)	Sigma-Aldrich (St. Louis, MO, USA)
6-Aminocaproic acid	Sigma-Aldrich (St. Louis, MO, USA)
Amino-Value 4000	Otsuka Pharmaceutical (Tokyo, Japan)
Arginine (Arg)	Kyowa Hakko Kogo Co., LTD (Tokyo, Japan)
Asparagine (Arg)	Sigma-Aldrich (St. Louis, MO, USA)
Aspartic acid (Asp)	Kyowa Hakko Kogo Co., LTD (Tokyo, Japan)
Boric acid	Wako Pure Chemical (Osaka, Japan)
Citric acid	Wako Pure Chemical (Osaka, Japan)
Citrulline (Cit)	Kyowa Hakko Kogo Co., LTD (Tokyo, Japan)
Coumarin 525	Exciton (Dayton, OH, USA)
Coumarin 545	Exciton (Dayton, OH, USA)
Cystine	Kyowa Hakko Kogo Co., LTD (Tokyo, Japan)
Dimethyloctadecylchlorosilane	Tokyo Chemical Industry CO., LTD. (Tokyo, Japan)
Ethanol (HPLC grade)	Kanto Chemical Co. (Tokyo, Japan)
Ethyl acetate (HPLC grade)	Kanto Chemical Co. (Tokyo, Japan)
4-Fluoro-7-nitro-2,1,3-benzoxadiazole (NBD-F)	Dojindo Laboratories (Kumamoto, Japan)
Glycine (Gly)	Kyowa Hakko Kogo Co., LTD (Tokyo, Japan)
Glutamine (Gln)	Kyowa Hakko Kogo Co., LTD (Tokyo, Japan)
Glutamic acid (Glu)	Sigma-Aldrich (St. Louis, MO, USA)

Heptylamine	Wako Pure Chemical (Osaka, Japan)
Hexylamine	Wako Pure Chemical (Osaka, Japan)
Histidine (His)	Kyowa Hakko Kogo Co., LTD (Tokyo, Japan)
Hydrochloric acid	Wako Pure Chemical (Osaka, Japan)
Isoleucine (Ile)	Kyowa Hakko Kogo Co., LTD (Tokyo, Japan)
Leucine (Leu)	Kyowa Hakko Kogo Co., LTD (Tokyo, Japan)
Lysine (Lys)	Kyowa Hakko Kogo Co., LTD (Tokyo, Japan)
Methanol (HPLC grade)	Wako Pure Chemical (Osaka, Japan)
Methionine (Met)	Kyowa Hakko Kogo Co., LTD (Tokyo, Japan)
Octylamine	Wako Pure Chemical (Osaka, Japan)
Ornithine (Orn)	Kyowa Hakko Kogo Co., LTD (Tokyo, Japan)
Pentylamine	Wako Pure Chemical (Osaka, Japan)
Phenylalanine (Phe)	Kyowa Hakko Kogo Co., LTD (Tokyo, Japan)
Proline (Pro)	Sigma-Aldrich (St. Louis, MO, USA)
Serine (Ser)	Kyowa Hakko Kogo Co., LTD (Tokyo, Japan)
Sodium citrate	Wako Pure Chemical (Osaka, Japan)
Sodium hydroxide	Wako Pure Chemical (Osaka, Japan)
Sodium perchlorate monohydrate	Wako Pure Chemical (Osaka, Japan)
Threonine (Thr)	Kyowa Hakko Kogo Co., LTD (Tokyo, Japan)
Toluene	Kanto Chemical Co. (Tokyo, Japan)
Trifluoroacetic acid (TFA)	Kanto Chemical Co. (Tokyo, Japan)
Type-H amino acid standard solution	Wako Pure Chemical (Osaka, Japan)
Tyrosine (Tyr)	Kyowa Hakko Kogo Co., LTD (Tokyo, Japan)
Valine (Val)	Sigma-Aldrich (St. Louis, MO, USA)
Water	Milli-Q system (Millipore, Bedford, MA, USA)

2.2 Experiment equipments

<HPLC system>

Pump	PU-1580, Jasco, Tokyo, Japan
Ternary gradient unit	LG-1580-02, Jasco, Tokyo, Japan
Degasser	DG-980-50, Jasco, Tokyo, Japan
Column oven	CO 631C, GL Sciences Inc., Tokyo, Japan
Fluorescence detector	FP-2025 Plus, Jasco, Tokyo, Japan
Integrator	807-IT, Tokyo, Japan

< Nexera UPLC system >

Pumps	LC-30AD, Shimadzu, Tokyo, Japan
Degasser	DGU-20A$_5$, Shimadzu, Tokyo, Japan
Column oven	CTO-30A, Shimadzu, Tokyo, Japan
Fluorescence detector	RF-20A, Shimadzu, Tokyo, Japan
System controller	CBM-20Alite, Shimadzu, Tokyo, Japan
Autosampler	SIL-30AC, Shimadzu, Tokyo, Japan

< Chip-LC system>

Pump	MP711, GL Sciences, Tokyo, Japan
Injector	Valco Instruments, Houston, TX

<Fluorescence microscopy system>

Inverted microscope	IX70, Olympus, Tokyo, Japan
Objective lens	UplanFL 4×, N.A. 0.13, PhL, Olympus
	UplanFL 20×, N.A. 0.13, PhL, Olympus
Lamp	A metal halide lamp
Excitation filter	BP460-490, Olympus
Dichroic mirror	505DRLP, Omega Optical, Brattleboro, VT
Emission filter	HQ 535m, Chroma Technology, Rockingham, VT
Camera	
	ORCA-ER CCD camera, Hamamatsu Photonics, Hamamatsu, Japan
Photomultiplier	
	H7421-40, Hamamatsu Photonics, Hamamatsu, Japan
Photocounter	PHC-2500, Scientex, Hamamatsu, Japan

Chapter 3. Analysis of amino acids with monolithic silica column

3.1 Introduction

Amino acids have attracted significant attention because they are involved in myriad biological activities, such as protein synthesis and regulation of many metabolic pathways [33]. The metabolite profiles of amino acids were reported to be useful in analyzing several diseases such as diabetes [35], inflammatory bowel disease [34], and Huntington's disease [36]. As a consequence, the development of a fast and accurate analytical method for the determination of amino acids in biological samples would be significant to facilitate the prediction, diagnosis, and understanding of diseases. Up to now, many determination methods for amino acids, such as HPLC-ultraviolet or fluorescence detection [38, 39], gas chromatography [40, 41], have been reported. Among these, the HPLC-fluorescence detection method is very popular, however, underivatized amino acids do not have the capability of fluorescence, except phenylalanine, tyrosine, and tryptophan; therefore, precolumn derivatization is necessary. Derivatization reagents such as 6-aminoquinolyl-N-hydroxysuccinimidyl carbamate (AQC) [42], 9-fluorenylmethyl chloroformate (FMOC) [43], and ortho-phthalaldehyde (OPA) [44, 45] were used. However, these reagents have some limitations, which include the formation of unstable derivatives, the extremely tedious derivatization procedure, and reactive interference. 4-Fluoro-7-nitro-2,1,3-benzoxadiazole (NBD-F) has been reported as the derivatization reagent for the determination of amino acids [46]. NBD-F has several merits such as a fast and efficient reaction with primary and secondary amino acids and a long wavelength of excitation and fluorescence, which leads to a relatively high sensitivity [47-50].

Recently, analytical methods requiring shorter analysis time are preferred,

however at least 30 min was usually required for analysis [51-53]. In order to achieve a fast analysis, some new types of columns were developed. Ultra-performance liquid chromatography (UPLC) utilizes smaller particles (below 2 μm) and higher pressure than the conventional HPLC, which leads to shorter analysis time, better resolution, and higher sensitivity. Although the amino acids can be analyzed in 10 min by using UPLC [54], special and expensive instruments are necessary.

In the past decade, a monolithic silica column as an alternative to the conventional particle packed column has been attracting more and more interests. Differing from the conventional column, a monolithic silica column is comprised of a single phase which is made of porous silica, having a distinctive bimodal pore structure: macropores and mesopores. The diameter of macropores is approximately 2 μm, and the total porosity of the monolithic silica column can reach up to 80%, which is about 2 times higher than that of the conventional column. These characteristics imbue the monolithic silica columns with high permeability and low flow resistance, leading to low column backpressure and high-speed separations. The diameter of mesopores is 13 nm, which can ensure a sufficient surface area for an efficient separation; additionally, fast mass transfer kinetics can also be achieved.

The aim of this study is to develop a fast HPLC method using monolithic silica columns for determining of amino acids derivatized with NBD-F. As a starting point, a monolithic silica column with a length of 250 mm was used for fast analysis of NBD-amino acids. Because a shorter column allows experiments to be performed at higher flow rates and reduces the analysis time, a 150-mm-long monolithic column was then used for analysis of NBD-amino acids in the biological samples within a much shorter analysis time.

3.2 Analysis of amino acids with a 250-mm-long monolithic silica column

3.2.1 Experimental section

3.2.1.1 Fluorescence derivatization

Twenty microliters of an amino acid solution and 20 µL of an internal standard solution (0.1 mM 6-aminocaproic acid) were added to 180 µL of 0.2 M borate buffer (pH 8.5). Then, 40 µL of 10 mM NBD-F was added to the mixture and heated to 60 °C for 5 min. After cooling the reaction mixture in ice water, 240 µL of 50 mM HCl solution was added to the reaction mixture. Ten microliters of the resultant solution was injected into the HPLC system.

3.2.1.2 Pretreatment of mouse plasma sample

Male C57/BL6 mice were anesthetized with diethyl ether. Blood samples were collected, transferred to a heparinized polyethylene tube and centrifuged at 3000 *g* for 10 min at 4 °C. The plasma fraction was separated and stored at -20 °C until the analysis. Forty µL of an internal standard solution (0.1 mM 6-aminocaproic acid), 160 µL of methanol, and 160 µL of acetonitrile were added to 40 µL of the mouse plasma sample. After the mixture was centrifuged at 3000 *g* for 5 min, 20 µL of the supernatant was evaporated to dryness under reduced pressure at 60 °C for 20 min. Then, the residue was added to 180 µL of 0.2 M borate buffer (pH 8.5). Forty microliters of 10 mM NBD-F was added and heated to 60 °C for 5 min. After cooling in ice water, 280 µL of 50 mM HCl solution was added to the reaction mixture.

3.2.1.3 HPLC conditions

The determination of NBD-amino acids was performed on an HPLC system. Fluorescence detection was performed at 530 nm with excitation at 470 nm. The separation column was MonoClad C18-HS (250 mm × 3 mm I.D., GL Sciences Inc.). Eluent A was water-acetonitrile-TFA (90:10:0.12, v/v/v); eluent B was water-acetonitrile-TFA (10:90:0.12, v/v/v). The gradient elution of the mobile phase is shown in Table 3-1. The column oven was maintained at 40 °C and the flow rate was

set at 1.4 mL/min.

3.2.1.4 Validation study

Calibration standards for amino acids with different concentrations (0, 0.5, 2.5, 5, 25, and 50 μM) were prepared from the stock solutions. Calibration curves were constructed by plotting the ratio of the peak heights of NBD-amino acids to the internal standard versus the injection amounts of the NBD-amino acids. The intra-day precision was determined by analyzing the plasma sample five times in the same day. The inter-day precision experiment was performed by analyzing the plasma sample once a day for five consecutive days. For the stability experiment, the same sample which was stored in 4 °C was analyzed for the second time in the fifth day. Recovery was assessed by the addition of 16.7, 33.3 and 66.7 μM standard amino acids to the mouse plasma samples.

3.2.2 Results and discussion

3.2.2.1 Optimization of the separation of 19 NBD-amino acids at the flow rate of 0.4 mL/min

First, the separation of 19 NBD-amino acids was performed at the flow rate of 0.4 mL/min in order to examine the separation efficiency of the monolithic silica column (MonoClad C18-HS). On the basis of the findings reported in our previous paper [46], two types of mobile phases, water-acetonitrile-TFA (90:10:0.08, v/v/v) and water-acetonitrile-TFA (10:90:0.08, v/v/v), were used for the gradient elution. However, NBD-arginine and NBD-OH, NBD-methionine and NBD-valine, and NBD-lysine and NBD-isoleucine could not be well separated (Figure 3-1). Hence, the concentration of TFA in the mobile phases, the gradient program, and the column temperature were optimized.

The concentration of TFA in the mobile phase was firstly investigated. It was found to have significant effects on the separations of NBD-arginine, NBD-OH, and NBD-aspartic acid. As shown in Figure 3-2, the separation of NBD-arginine and NBD-OH improved with the increase of the concentration of TFA, while the separation of NBD-OH and NBD-aspartic acid had worsened. Therefore, the concentration of TFA in the mobile phase was set as 0.12 % in the following experiments.

The effects of column temperature from 30 to 42.5 °C on the separations (NBD-OH and NBD-aspartic acid, NBD-methionine and NBD-valine, NBD-lysine and NBD-isoleucine) were also examined. As indicated in Figure 3-3, NBD-OH and NBD-aspartic acid had a better separation at lower temperature, while the separations of NBD-methionine and NBD-valine, NBD-lysine and NBD-isoleucine improved as the temperature increased. Therefore, the column temperature was set as 40 °C.

Accordingly, the optimum conditions were determined as follows: Eluent A was water-acetonitrile-TFA (90:10:0.12, v/v/v); eluent B was water-acetonitrile-TFA (10:90:0.12, v/v/v). The gradient elution of the mobile phase is shown in Table 3-2. The column oven was maintained at 40 °C. As can be seen in Figure 3-4, the 19 NBD-amino acids were well separated within 80 min under the optimum condition. This result indicates that the separation efficiency of monolithic silica column is comparable to that of conventional particle-packed columns.

3.2.2.2 Comparison of properties of the monolithic silica column at different flow rates

The monolithic silica column was made from porous cross-linked silica, and its total porosity can reach 80% or higher. The large pore size/skeleton size ratio and its high porosity can lead to high column efficiencies. Therefore, when compared to a conventional particle-packed column, the monolithic column enabled a relatively high flow rate analysis without affecting the column performance. In order to investigate the properties of the monolithic column (Monoclad C18-HS), 7 NBD-amino acids

(histidine, asparagine, glutamine, serine, arginine, aspartic acid, and glycine) were analyzed at several flow rates (0.4, 0.8, 1.2, 1.4, and 1.6 mL/min) with an isocratic elution of the mobile phase (water-acetonitrile-TFA (90:10:0.12, v/v/v)). The chromatograms of 7 NBD-amino acids that were analyzed at several flow rates are given in Figure 3-5.

The chromatographic parameters, such as the theoretical plate number, resolution factor, retention time, and column pressure, were calculated for each flow rate. As can be seen from Table 3-3, with an increase in the flow rate, the retention time decreased, while the column pressure increased. Although the theoretical plate number of NBD-glycine decreased slightly with an increase in the flow rate, the resolution factor seemed to have no significant change. Considering the high efficiency and acceptable column pressure, the following experiment was performed at a flow rate of 1.4 mL/min.

3.2.2.3 Optimization of the separation of 19 NBD-amino acids at the flow rate of 1.4 mL/min

First, the separation of the 19 NBD-amino acids at the flow rate of 1.4 mL/min was performed with the gradient program on the basis of the results obtained in the case of the flow rate of 0.4 mL/min (Table 3-2). However, NBD-lysine and NBD-isoleucine could not be well separated. Hence, the gradient program was changed to improve the separation of NBD-lysine and NBD-isoleucine. On the basis of the experimental results, the gradient program was confirmed as shown in Table 3-1. A representative chromatogram of 19 NBD-amino acids at the flow rate of 1.4 mL/min is shown in Figure 3-6 (a).

3.2.2.4 Validation of the analytical method

As shown in Table 3-4, the limits of detection (signal-to-noise ratio = 3) for the individual NBD-amino acids were in the range of 4.27 to 53.4 fmol, and the limits of

quantitation (signal-to-noise ratio = 10) for the individual amino acids were in the range of 14.2 to 178 fmol. These values are comparable to our previous data obtained by using a conventional particle-packed column. The proposed method was more sensitive than the methods using other fluorescent derivatization reagents [42-45].

Calibration curves were linear over the range of 200 fmol to 20 pmol with correlation coefficients of 0.997 or better for each amino acid. As shown in Table 3-5, the obtained RSD values were 0.68%–4.9% for the intra-day precision (n = 5), and those for the inter-day precision were 0.71%–5.2% (n = 5). In the stability test, the values ranging from 89.6 to 101.6 % showed that NBD-amino acids were stable after stored in 4 °C for 5 days. The recoveries for all of the amino acids were 88.5%–115%, which are depicted in Table 3-6.

3.2.2.5 Application to mouse plasma sample

As an application of the proposed method, the determination of amino acids in the mouse plasma was carried out. The chromatogram obtained from the mouse plasma is shown in Figure 3-6 (b). The concentration of amino acids in the mouse plasma is given in Table 3-7. Most values were in good agreement with the data reported in the literature [46]. However, the concentrations of aspartic acid and cystine were found to be considerably higher than normal values. The concentrations of cystine and ornithine were known to be high in the plasma samples; moreover, the peaks of NBD-aspartic acid and NBD-cystine were found to be respectively overlapped with those of NBD-citrulline and NBD-ornithine. Hence, the concentrations of aspartic acid and cystine in mouse plasma could not be determined. Further studies are necessary to quantify all of the amino acids, including aspartic acid and cystine.

3.3 Analysis of amino acids with a 150-mm-long monolithic silica column

In section 3.2, a fast HPLC method using a 250-mm-long monolithic silica column for

the determination of 19 NBD-amino acids was developed. However, the concentrations of aspartic acid and cystine in mouse plasma could not be determined. Further studies are necessary to quantify all of the amino acids, including aspartic acid and cystine. In mammals, the adrenal glands are endocrine glands which are responsible for releasing hormones including catecholamines (such as epinephrine and norepinephrine) and corticosteroids (such as cortisol) [55, 56]. Past research has uncovered a number of biological activities of amino acids in adrenal glands. Leu and Met are essential in the secretion of adrenocortical hormones [57]; catecholamines are synthesized from Tyr in adrenal glands [58, 59]. However, up to now, the determination of amino acids in the adrenal glands has seldom been reported. Hence, the proposed method was applied to determine the amino acids in adrenal sample as well as mouse plasma. Because a shorter column allows experiments to be performed at higher flow rates and reduces the analysis time, a 150-mm-long monolithic column was used for analysis of NBD-amino acids in the biological samples within a much shorter analysis time.

3.3.1 Experimental section

3.3.1.1 Fluorescence derivatization procedure and pretreatment of mouse plasma sample

These were performed according to the work described in section 3.2.1.

3.3.1.2 Pretreatment of mouse adrenal sample

Male C57/BL6 mice were anesthetized with diethyl ether and the adrenal glands were removed and homogenized with four volumes of 0.4 mol/L perchloric acid containing 0.05% (w/v) EDTA-2Na. The tissue homogenates were centrifuged at 15000 × g for 5 min at 4 ˚C. The supernatant was stored at -80 ˚C until the assay. Ten microliters of supernatant and 40 μL of internal standard solution (0.1 mM 6-aminocaproic acid)

were added to 180 μL of 0.2 M borate buffer (pH 8.5). Then 40 μL of 10 mM NBD-F was added and heated to 60 ˚C for 5 min, and 230 μL of 0.05 M HCl solution was added into the sample in order to stop the reaction.

3.3.1.3 Chromatographic conditions

The separation was performed using a MonoClad C18-HS (150 mm × 3 mm I.D., GL Sciences, Tokyo, Japan). The fluorescence detention was carried out at an emission wavelength of 530 nm with excitation at 470 nm. Mobile phase A was 25 mM citrate buffer containing 25 mM $NaClO_4$ (pH 5.5), and mobile phase B was 25 mM citrate buffer containing 25 mM $NaClO_4$ (pH 5.5)/acetonitrile (50/50, v/v). The gradient elution of the mobile phase was shown in Table 1. The temperature of the column oven changed linearly from 30 to 49 ˚C within 10 min. The flow rate was kept at 2.0 mL/min.

3.3.1.4 Method validation

Standard stock solutions were prepared by dissolving amino acids in 0.1 M HCl solution. After the fluorescent derivatization reactions, NBD-amino acid solutions with different concentrations (0.2, 2, 10, 40, and 200 μM) were injected into the HPLC system to make the calibration. The linear regression of the calibration curves were analyzed by plotting the ratio of the peak heights of NBD-amino acids to that of the internal standard versus the injection amounts of the NBD-amino acids.

In order to determine the accuracy of this method, the standard amino acid solutions with different concentrations (0.2, 2, 10, 40, and 200 μM) were added into the mouse plasma sample. Accordingly, the calibration curves were obtained by the method depicted previously. The accuracies were obtained by calculating the ratio of slopes of the standards-spiked plasma sample to the standard amino acid solutions. The precision of the proposed method was investigated by analyzing the same mouse plasma sample for five times in one day and on five consecutive days.

3.3.2 Results and discussion

3.3.2.1 Optimization of chromatographic conditions

Considering the faster analysis time and the pressure limits of the monolithic silica column, the following experiments were performed at a flow rate of 2 mL/min.

In order to achieve a good separation in a shorter analysis time, the chromatographic conditions (including mobile phase and temperature) were optimized. In this study, citrate buffer was chosen for a better separation. However, the peaks of NBD-His, NBD-Gly, and NBD-Gln were overlapped. In some studies, $NaClO_4$ as a mobile phase modifier was added to optimize the separation of amino acids [60, 61]. Hence, the effects of $NaClO_4$ on the separation of NBD-His, NBD-Gly, and NBD-Gln were examined (Figure 3-7). After further optimization, better separation was achieved by adding 25 mM $NaClO_4$ to the mobile phase.

Temperature was found to have significant effects on the separation of NBD-amino acids. The relationship between the column temperature and the retention times of several NBD-amino acids is depicted in Figure 3-8. NBD-Asn and NBD-OH displayed better separation at 30 ˚C, while NBD-Arg and NBD-Ala were well separated at 40 ˚C. Besides, increase of the column temperature is an effective way to save analysis time. Therefore, a gradient program for the temperature was utilized in this experiment. Accordingly, the optimum chromatographic conditions were as follows: Eluent A was 25 mM citrate buffer (pH 5.5) containing 25 mM $NaClO_4$, and eluent B was 25 mM citrate buffer (pH 5.5) containing 25 mM $NaClO_4$/acetonitrile (50/50, v/v). The gradient elution of the mobile phase was as follows: 95-76.2 % (A) from 1 to 1.8 min, 76.2 % (A) from 1.8 to 2.1 min, 76.2-68.1 % (A) from 2.1 to 3.0 min, 68.1-50 % (A) from 3.0 to 3.1 min, 50 % (A) from 3.1 to 9.5 min, 50-0 % (A) from 9.5 to 9.6 min, 0 % (A) from 9.6 to 10.0 min . The temperature of the column oven changed from 30 to 49 ˚C linearly within 10 min. The representative chromatogram of 21 NBD-amino acids under the optimum conditions is shown in

Figure 3-9 (a). The analysis was performed in only 10 min, which is comparable to other studies using UPLC and/or MS.

3.3.2.2 Validation of the proposed method

As shown in Table 3-8, the limits of detection (LOD, signal-to-noise ratio = 3) for the individual NBD-amino acids were in the range of 3.2 to 134 fmol, and the limits of quantification (LOQ, signal-to-noise ratio = 10) were in the range of 10.8 to 445 fmol. The calibration curves for NBD-amino acids showed linearity in the range of 40 fmol to 40 pmol. The coefficients of correlation were 0.996 or higher for each NBD-amino acid.

Table 3-9 showed the data of precision and accuracy for the determination of NBD-amino acids. The intra-day precision (n = 5) for each NBD-amino acid ranged from 0.37 to 4.7 %, and inter-day precision (n = 5) was in the range of 0.75 to 4.8 %. The accuracies for all NBD-amino acids varied between 91.2 to 110 %. These results indicate that the proposed method could be applied for the determination of amino acids in biological samples.

3.3.2.3 Determination of amino acids in mouse plasma and adrenal sample

The proposed method was applied to determine the amino acids in mouse plasma and adrenal sample. Figure 3-9 (b) and (c) shows the chromatograms which were respectively obtained from mouse plasma and adrenal sample. The concentrations of amino acids are presented in Table 3-10. The values obtained in the present study are in good agreements with the previous reports [38, 43, 62, 63].

3.4 Conclusions

Fast HPLC methods using monolithic silica columns with different lengths for the determination of NBD-amino acids were developed. When the 250-mm-long column

was used, the analysis of the mouse plasma sample could be completed in 18 min; however, the concentrations of Asp and cystine in mouse plasma could not be determined. After using the monolithic column with a length of 150 mm, the analysis of 21 NBD-amino acids was successfully performed in 10 min. Without any special requirements in terms of instruments or high costs, the developed methods can be used for routine analyses using conventional instruments in common laboratories and will contribute to the investigation of the important role of amino acids in the field of life sciences.

Figures

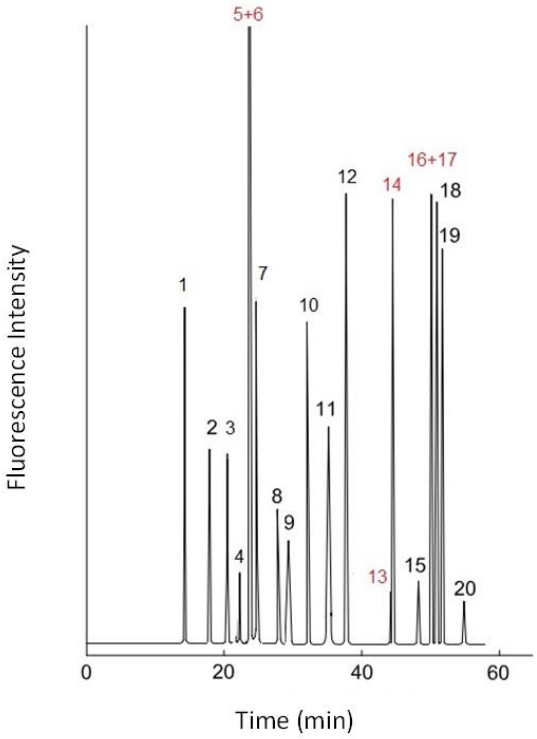

Figure 3-1. Chromatogram of 19 NBD-amino acids solution obtained at a flow rate of 0.4 mL/min (before optimization of chromatographic conditions).

Peaks in the chromatogram: 1, NBD-histidine; 2, NBD-asparagine; 3, NBD-glutamine; 4, NBD-serine; 5, NBD-arginine; 6, NBD-OH; 7, NBD-aspartic acid; 8, NBD-glycine; 9, NBD-glutamic acid; 10, NBD-threonine; 11, NBD-alanine; 12, NBD-proline; 13, NBD-methionine; 14, NBD-valine; 15, NBD-cystine; 16, NBD-lysine; 17, NBD-isoleucine; 18, NBD-leucine; 19, NBD-phenylalanine; and 20, NBD-tyrosine.

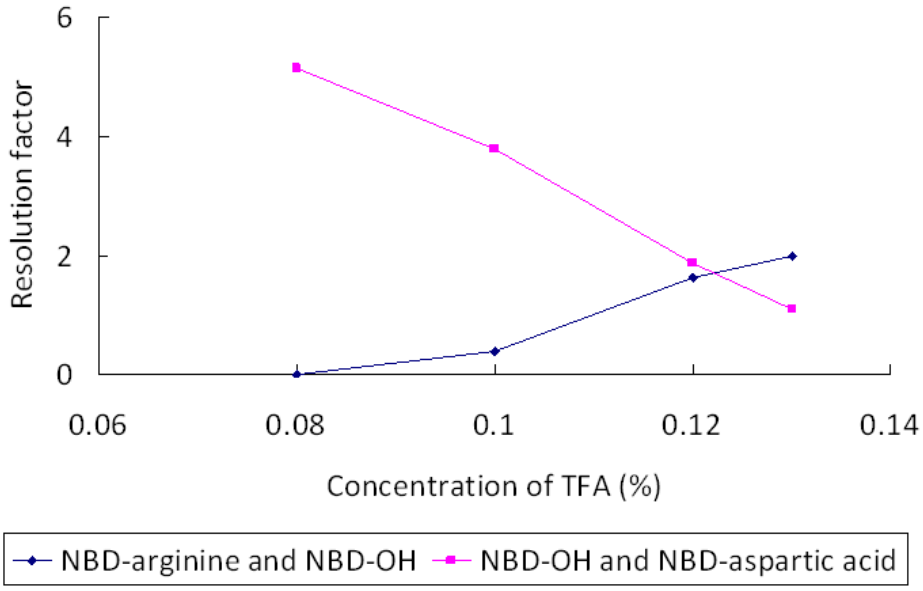

Figure 3-2. Relationship between the resolution factors of two pairs of peaks (NBD-arginine and NBD-OH, NBD-OH and NBD-aspartic acid) and the concentration of TFA in the mobile phase

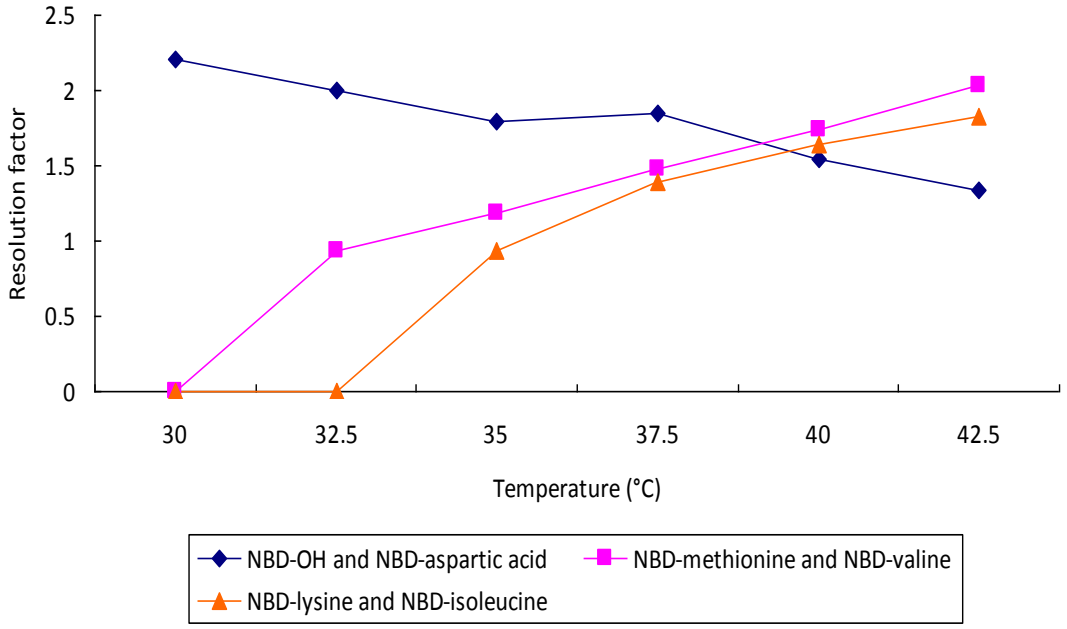

Figure 3-3. Relationship between the resolution factors of three pairs of peaks (NBD-OH and NBD-aspartic acid, NBD-methionine and NBD-valine, NBD-lysine and NBD-isoleucine) and column temperature

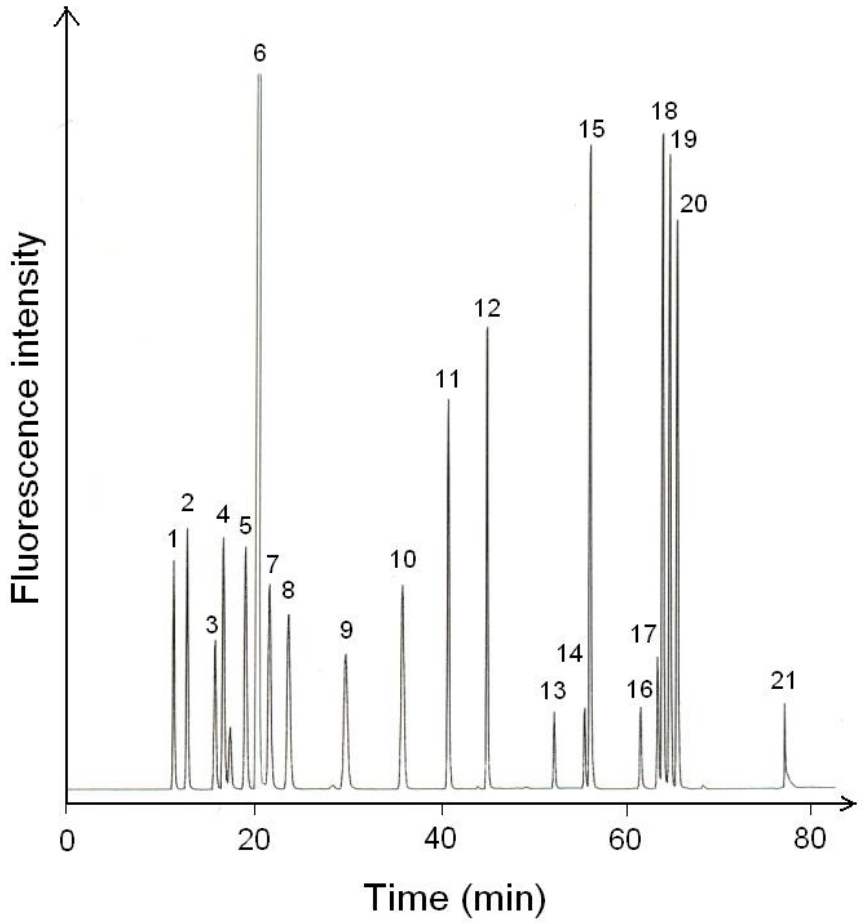

Figure 3-4. Chromatogram of 19 NBD-amino acids solution obtained at a flow rate of 0.4 mL/min.

Peaks in the chromatogram: 1, NBD-histidine; 2, NBD-asparagine; 3, NBD-glutamine; 4, NBD-serine; 5, NBD-arginine; 6, NBD-OH; 7, NBD-aspartic acid; 8, NBD-glycine; 9, NBD-glutamic acid; 10, NBD-threonine; 11, NBD-alanine; 12, NBD-proline; 13, NBD-6-aminocaproic acid (internal standard); 14, NBD-methionine; 15, NBD-valine; 16, NBD-cystine; 17, NBD-lysine; 18, NBD-isoleucine; 19, NBD-leucine; 20, NBD-phenylalanine; and 21, NBD-tyrosine.

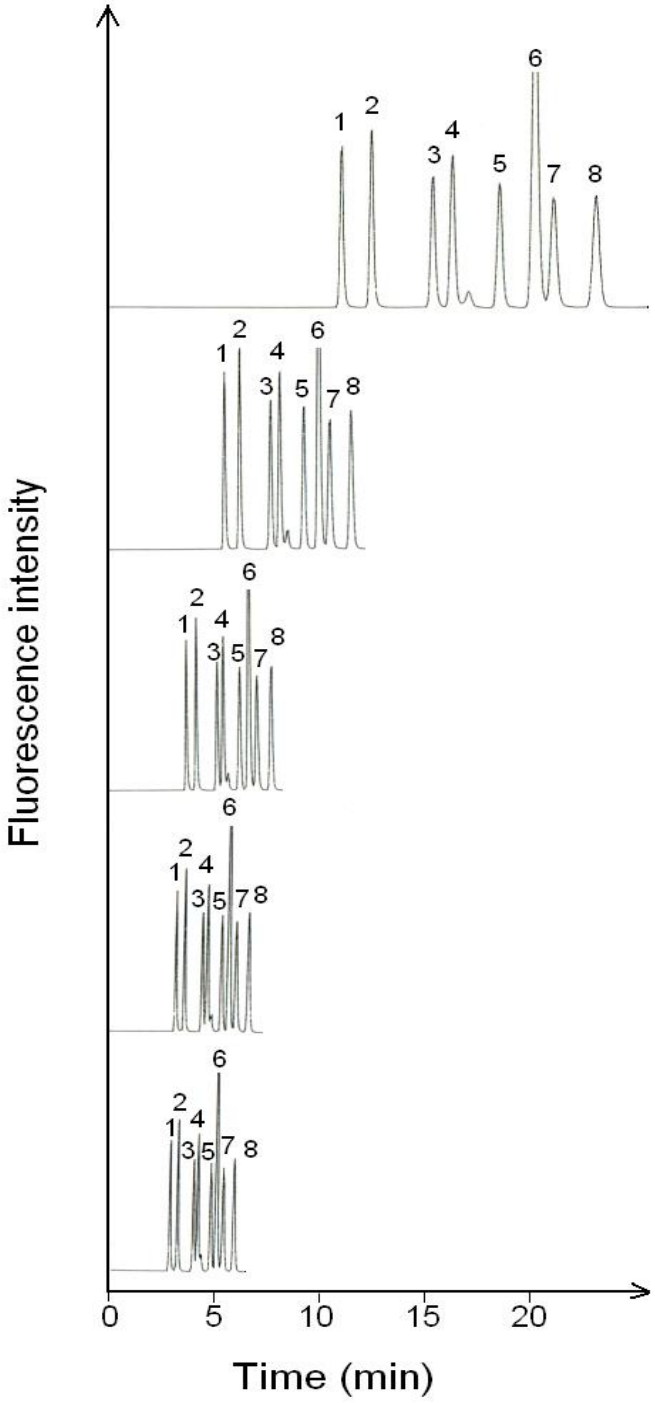

Figure 3-5. Chromatogram of 7 NBD-amino acids obtained at the flow rates of 0.4, 0.8, 1.2, 1.4, and 1.6 mL/min.

Peaks in the chromatogram: 1, NBD-histidine; 2, NBD-asparagine; 3, NBD-glutamine; 4, NBD-serine; 5, NBD-arginine; 6, NBD-OH; 7, NBD-aspartic acid; and 8, NBD-glycine.

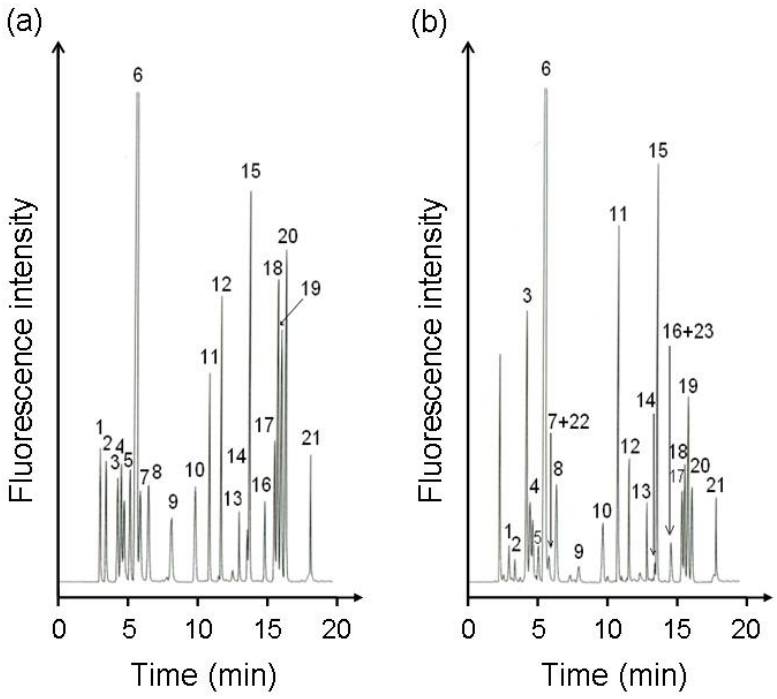

Figure 3-6. Chromatogram (a) of 19 NBD-amino acid solution and (b) obtained from mouse plasma samples.

Peaks in the chromatogram: 1, NBD-histidine; 2, NBD-asparagine; 3, NBD-glutamine; 4, NBD-serine; 5, NBD-arginine; 6, NBD-OH; 7, NBD-aspartic acid; 8, NBD-glycine; 9, NBD-glutamic acid; 10, NBD-threonine; 11, NBD-alanine; 12, NBD-proline; 13, NBD-6-aminocaproic acid (internal standard); 14, NBD-methionine; 15, NBD-valine; 16, NBD-cystine; 17, NBD-lysine; 18, NBD-isoleucine; 19, NBD-leucine; 20, NBD-phenylalanine; 21, NBD-tyrosine; 22, NBD-citrulline; and 23, NBD-ornithine.

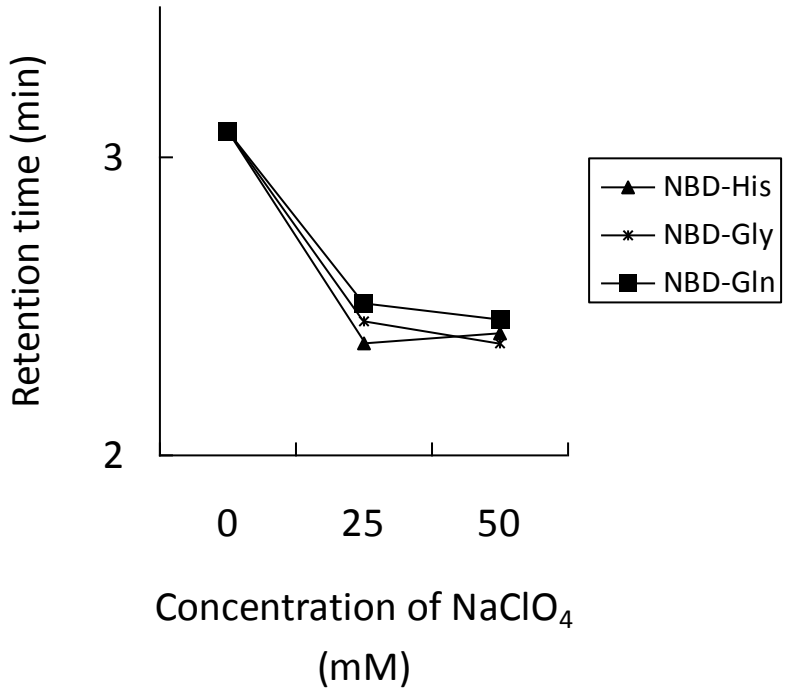

Figure 3-7. Relationship between concentration of $NaClO_4$ and the retention times of NBD-His, NBD-Gly, and NBD-Gln.

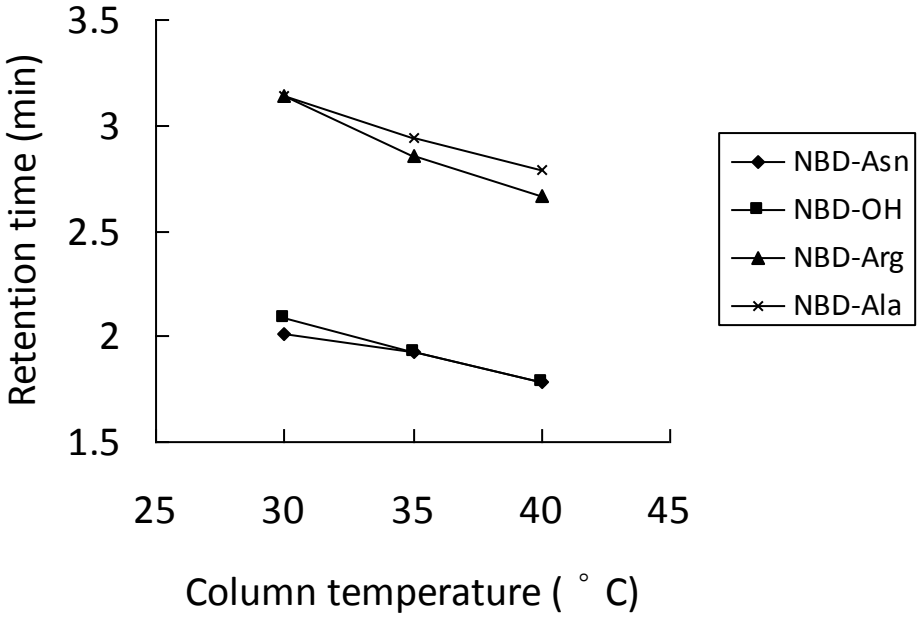

Figure 3-8. Relationship between column temperature and the retention times of NBD-Asn, NBD-OH, NBD-Arg, and NBD-Ala.

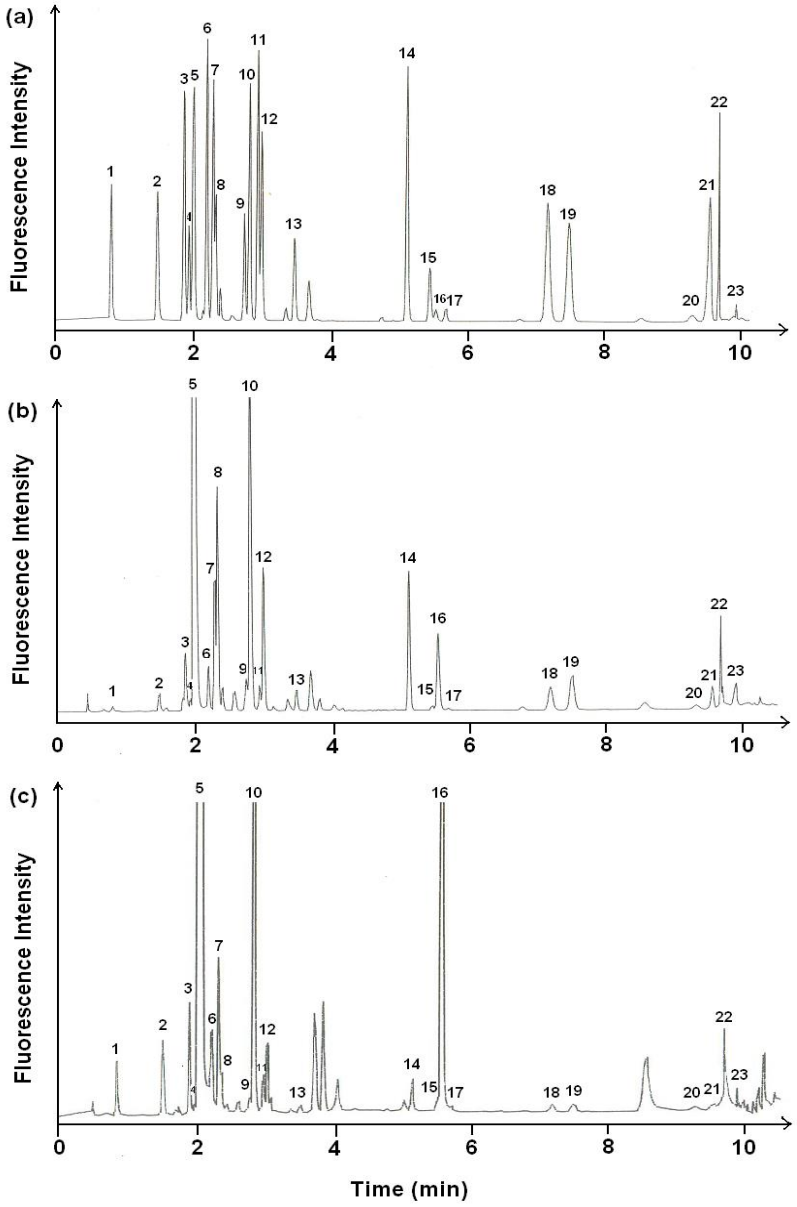

Figure 3-9. Chromatogram (a) of 21 NBD-amino acid solution and (b) obtained from mouse plasma samples and (c) adrenal sample. Peaks in the chromatogram: 1, NBD-aspartic acid; 2, NBD-glutamic acid; 3, NBD-serine; 4, NBD-asparagine; 5, NBD-OH; 6, NBD-histidine; 7, NBD-glycine; 8, NBD-glutamine; 9, NBD-citrulline; 10, NBD-threonine; 11, NBD-arginine; 12, NBD-alanine; 13, NBD-proline; 14, NBD-valine; 15, NBD-methionine; 16, NBD-6-aminocaproic acid (internal standard); 17, NBD-cystine; 18, NBD-isoleucine; 19, NBD-leucine; 20, NBD -ornithine; 21, NBD-phenylalanine; 22, NBD-lysine; and 23, NBD-tyrosine.

Tables

Table 3-1. Gradient elution program used for analysis of NBD-amino acids

Time (min)	Composition (%)[a]	
	Eluent A	Eluent B
0	100	0
7.1	100	0
11	50	50
15.9	50	50
16	0	100
18	0	100
18.1	100	0

[a] All the compositions of the solvents were changed linearly.

Table 3-2. Gradient elution program used for analysis of NBD-amino acids at a flow rate of 0.4 mL/min

Time (min)	Composition [a] (%)	
	Eluent A	Eluent B
0	100	0
25	100	0
60	50	50
70	50	50
71	0	100
80	0	100
81	100	0

[a] All the compositions of the solvents were changed linearly.

Table 3-3. Chromatographic parameters obtained at different flow rates

Flow rate (mL/min)	Theoretical plate number (NBD-glycine)	Rs (NBD-OH and NBD-aspartic acid)	Retention time of NBD-glycine (min)	Column pressure (bar)
0.4	22800	1.8	22.8	62
0.8	20700	1.9	11.4	126
1.2	20200	1.9	7.58	190
1.4	19000	1.9	6.51	223
1.6	18300	1.6	5.75	256

Table 3-4. Limits of detection and limits of quantitation of individual NBD-amino acids

Amino acid	Limits of detection (fmol)	Limits of quantitation (fmol)	Amino acid	Limits of detection (fmol)	Limits of quantitation (fmol)
His	7.09	23.6	Pro	4.67	15.6
Asn	14.1	46.9	Met	33.3	111
Gln	53.4	178	Val	2.94	9.80
Ser	23.8	79.3	Cystine	7.70	25.7
Arg	12.1	40.4	Lys	14.8	49.3
Asp	9.09	30.3	Ile	4.27	14.2
Gly	4.52	15.1	Leu	4.40	14.7
Glu	17.8	59.2	Phe	4.97	16.6
Thr	12.1	40.4	Tyr	10.3	34.2
Ala	3.70	12.2			

Table 3-5. Precisions and stabilities of the proposed method for the determination of mouse plasma

Amino acid	Intra-day precision (%) (n = 5)	Inter-day precision (%) (n = 5)	Stability (%)	Amino acid	Intra-day precision (%) (n = 5)	Inter-day precision (%) (n = 5)	Stability (%)
His	3.1	2.6	96.2	Pro	0.68	0.75	94.1
Asn	4.7	2.4	98.0	Met	4.9	2.3	91.7
Gln	2.1	3.2	94.5	Val	1.6	2.8	94.7
Ser	2.1	1.0	101.2	Lys	4.0	2.3	101.6
Arg	2.1	2.6	95.3	Ile	0.70	1.9	92.9
Gly	1.6	0.72	95.2	Leu	0.95	2.1	96.9
Glu	1.8	0.71	94.8	Phe	2.1	4.3	99.2
Thr	4.0	2.6	97.7	Tyr	4.8	5.2	89.6
Ala	0.92	1.2	99.8				

Table 3-6. Accuracy data for the determination of mouse plasma

Amino acid	Amount added (μM)	Recovery (%)	Amino acid	Amount added (μM)	Recovery (%)
	16.7	94.4		16.7	102
His	33.3	92.6	Pro	33.3	97.7
	66.7	90.4		66.7	108
	16.7	94.8		16.7	99.8
Asn	33.3	91.3	Met	33.3	108
	66.7	97.4		66.7	95.6
	16.7	103		16.7	98.8
Gln	33.3	115	Val	33.3	92.0
	66.7	103		66.7	108
	16.7	98.8		16.7	90.0
Ser	33.3	92.6	Lys	33.3	101
	66.7	110		66.7	93.6
	16.7	88.5		16.7	106
Arg	33.3	96.6	Ile	33.3	95.4
	66.7	102		66.7	108
	16.7	100		16.7	105
Gly	33.3	106	Leu	33.3	109
	66.7	105		66.7	110
	16.7	101		16.7	93.7
Glu	33.3	110	Phe	33.3	104
	66.7	110		66.7	90.0
	16.7	110		16.7	98.8
Thr	33.3	104	Tyr	33.3	108
	66.7	97.9		66.7	105
	16.7	95.0			
Ala	33.3	105			
	66.7	105			

Table 3-7. Concentrations of amino acids in mouse plasma

Amino acid	Concentrations[a] (μM) (n = 3)	Amino acid	Concentrations (μM) (n = 3)
His	46.0 ± 9.2	Pro	60.1 ± 9.0
Asn	18.2 ± 2.6	Met	23.2 ± 3.1
Gln	503 ± 62	Val	148 ± 20
Ser	81.5 ± 11.4	Lys	150 ± 21
Arg	26.7 ± 3.7	Ile	59.6 ± 8.0
Gly	145 ± 23	Leu	117 ± 16
Glu	25.5 ± 2.7	Phe	36.9 ± 6.4
Thr	46.6 ± 5.0	Tyr	94.6 ± 7.7
Ala	244 ± 23		

[a] The concentrations are presented as mean ± standard deviation.

Table 3-8. Limit of Detection (S/N=3) and Limit of Quantitation (S/N=10) of individual NBD-amino acids

Amino acid	Limit of Detection (fmol)	Limit of Quantitation (fmol)	Amino acid	Limit of Detection (fmol)	Limit of Quantitation (fmol)
Asp	11.7	39.0	Pro	3.2	10.8
Glu	14.8	49.3	Val	9.5	31.8
Ser	3.7	12.2	Met	50.1	167
Asn	9.4	31.2	Cystine	20.3	67.8
His	13.4	44.5	Ile	18.8	62.7
Gly	3.5	11.5	Leu	21.1	70.3
Gln	3.9	13.2	Orn	57.2	191
Cit	8.4	27.9	Phe	25.0	83.4
Thr	7.3	24.2	Lys	10.5	35.1
Arg	8.9	29.9	Tyr	19.0	63.6
Ala	6.4	21.5			

Table 3-9. Precisions of the proposed method for the determination of mouse plasma

Amino acid	Intra-day precision (%) (*n*=5)	Inter-day precision (%) (*n*=5)	Accuracy (%)	Amino acid	Intra-day precision (%) (*n*=5)	Inter-day precision (%) (*n*=5)	Accuracy (%)
Asp	2.17	4.31	100.2	Pro	1.43	0.752	105.8
Glu	1.92	3.32	102.3	Val	0.79	2.25	94.0
Ser	0.86	2.38	102.2	Met	2.29	2.37	106.0
Asn	2.77	3.79	91.8	Cystine	1.32	2.28	94.2
His	2.77	4.64	95.8	Ile	0.37	2.49	105.2
Gly	2.42	3.94	94.8	Leu	0.53	1.31	95.2
Gln	2.46	4.51	91.2	Orn	3.55	1.94	91.5
Cit	1.84	4.17	94.7	Phe	0.92	1.27	92.0
Thr	1.51	4.81	94.3	Lys	4.60	3.06	95.4
Arg	1.61	2.20	109.8	Tyr	4.66	2.65	95.3
Ala	0.83	4.34	93.0				

Table 3-10. Concentrations of amino acids in mouse plasma sample and adrenal gland sample

Amino acid	Concentrations in mouse plasma sample (μM) (n = 3)	Concentrations in adrenal sample (pmol/mg tissue) (n = 3)	Amino acid	Concentrations in mouse plasma sample (μM) (n = 3)	Concentrations in adrenal sample (pmol/mg tissue) (n = 3)
Asp	2.93 ± 0.36	228±18.2	Pro	72.0 ± 8.25	134±6.72
Glu	33.6 ± 3.96	286±37.1	Val	156 ± 21.8	114±8.00
Ser	57.0 ± 4.42	173±36.0	Met	17.1 ± 2.73	230±20.7
Asn	13.6 ± 1.27	81±6.45	Cystine	46.3 ± 6.29	114±9.01
His	52.5 ± 4.84	333±20.0	Ile	69.3 ± 8.34	33±2.29
Gly	163 ± 25.9	214±29.3	Leu	102 ± 8.87	39±5.10
Gln	390 ± 48.7	70±7.05	Orn	65.6 ± 6.02	298±23.9
Cit	37.6 ± 4.81	131±11.8	Phe	46.6 ± 4.98	35±4.26
Thr	142 ± 25.1	1193±143	Lys	176 ± 13.4	223±34.5
Arg	28.6 ± 2.13	78±8.56	Tyr	103 ± 9.23	63±9.68
Ala	182 ± 20.7	88±9.29			

Chapter 4. Analysis of amino acids with core-shell particle column

4.1 Introduction

In Chapter 3, the analysis of NBD-amino acids was achieved in 10 min by using a monolithic silica column. However, during the experiments, column temperature gradient was used and column pressure was near the limitations due to high flow rate, which showed that it has been the limit of monolithic silica column. Therefore, another new type of column, core-shell particle column packing with core-shell particles (solid cores with surrounding porous silica shells), was considered. This semi-porous silica column provides a shorter diffusion path for a solute to minimize peak broadening at a high flow rate, which ensures that the efficiency is comparable with the column packing with fully porous sub-2 μm partiles. Besides, because it was surrounded with porous silica shells, it has a high permeability and low column backpressure, which allows high speed separations. According to the van Deemter equation, core-shell particle columns afford higher separation efficiency than monolithic silica columns [22, 23]. Hence, amino acids analysis using a core-shell particle column should be faster than using a monolithic silica column.

In this study, a core-shell particle column was applied for the determination of amino acids derivatized with 4-fluoro-7-nitro-2,1,3-benzoxadiazole (NBD-F), and a mouse plasma sample was analyzed to assess the method's feasibility.

4.2 Experimental section

4.2.1 Sample preparation

The preparation of mouse plasma sample and the derivatization procedure were according to the previous study in Chapter 3.

4.2.2 Chromatographic conditions

Mobile phase A was water/acetonitrile/TFA (90:10:0.12, v/v/v), and mobile phase B was water/acetonitrile/TFA (10:90:0.12, v/v/v). The gradient elution program of the mobile phases was as follows: 95 % (A) from 0 to 2.7 min, 95-63 % (A) from 2.7 to 3.6 min, 63 % (A) from 3.6 to 5.8 min, 63-0 % (A) from 5.8 to 6.0 min, 0 % (A) from 6.0 to 7.0 min, and 0-95 % (A) from 7.0 to 7.1 min. The column oven was kept at 45°C. The analysis was carried out at a flow rate of 1.0 mL/min.

The performances of the following three columns were compared: (1) Kinetex C18-100A column, (2) Inertsil ODS-4 column (150 mm × 3 mm I.D., 5 μm, GL Sciences, Tokyo, Japan), and (3) MonoClad C18-HS (150 mm × 3 mm I.D., GL Sciences). Isocratic elution was conducted at linear velocities ranging from 0.24 to 2.4 mm/s. The mobile phase was water/acetonitrile/TFA (86:14:0.12, v/v/v), and the column oven was set at 45°C.

4.3 Results and discussion

4.3.1 Comparison of van Deemter curves obtained by conventional particle-packed column, monolithic silica column, and core-shell particle column

The performances of three types of columns ((1) Inertsil ODS-4 column (150 mm × 3 mm I.D., 5 μm, GL Sciences, Tokyo, Japan), (2) MonoClad C18-HS (150 mm × 3 mm I.D., GL Sciences), and (3) Kinetex C18-100A column) were compared. Isocratic elution was carried out at linear velocities ranging from 0.24 to 2.4 mm/s. Water/acetonitrile/TFA (86:14:0.12, v/v/v) was utilized as the mobile phase, and the column oven was kept at 45 °C.

The van Deemter curves of NBD-Ser by the three columns were plotted as to

analyze the separation efficiencies. The experiments were performed with linear velocities in the range of 0.24 and 2.4 mm/s. As shown in Figure 4-1, the minimal theoretical plate height of NBD-Ser and NBD-Arg using the core-shell particle column was 5.0 and 5.1 μm, which was only half of the values obtained by the conventional particle-packed column (10.4 and 10.2 μm) and monolithic silica column (10.2 and 11.2 μm). For the conventional particle-packed column, the theoretical plate height increased to 16.2 μm when the linear velocity reached 2.4 mm/s. However, for the core-shell particle and monolithic silica columns, the theoretical plate height did not vary with an increase in the linear velocity. The van Deemter plotting curves for the other NBD-amino acids also showed similar trends, which indicates that the increase of the flow rate had little effect on separation for the core-shell particle column. Based on the van Deemter curves, the core-shell particle column have higher separation efficiencies comparing with conventional particle-packed column and monolithic silica column.

4.3.2 Chromatographic properties of core-shell particle column at different flow rates

Six NBD-amino acids (His, Asn, Gln, Ser, Arg, and Cit) were separated under different flow rates ranging from 0.1 to 1.0 mL/min with an isocratic elution for the investigation of the properties of core-shell particle column (Figure 4-2). The chromatographic parameters (theoretical plate number, theoretical plate height, resolution factor, retention time, and column pressure) were calculated. As presented in Table 4-1, with the increasing of the flow rates, the elution of NBD-Arg became faster, while the theoretical plate number, theoretical plate height and resolution factor didn’t change significantly. In order to keep high separation efficiency for a faster analysis with consideration of the limitation of the column pressure, the following experiments were performed under the flow rate of 1.0 mL/min.

4.3.3 Optimization of chromatographic conditions

Water/acetonitrile containing TFA were used as mobile phases based on our previous research [62]. First, the effects of the column temperature, ranging from 30 to 45°C, on the separation were investigated. With an increase in temperature, the analysis time became shorter without the loss of separation efficiency, and the column pressure was significantly decreased. For instance, the retention time of NBD-glutamine was shortened from 6.17 to 4.20 min, and the theoretical plate number decreased from 6900 to 6000, without significant change. Considering the limitations for the column temperature, the column temperature was kept as 45 °C in the following experiments. Then the gradient elution program was optimized to analyze the 21 NBD-amino acids. The Mobile phase A was water/acetonitrile/TFA (90:10:0.12, v/v/v), and mobile phase B was water/acetonitrile/TFA (10:90:0.12, v/v/v). The gradient elution program of the mobile phases was: 95 % (A) from 0 to 2.7 min, 95-63 % (A) from 2.7 to 3.6 min, 63 % (A) from 3.6 to 5.8 min, 63-0 % (A) from 5.8 to 6.0 min, 0 % (A) from 6.0 to 7.0 min, and 0-95 % (A) from 7.0 to 7.1 min. The column oven was kept at 45°C. The analysis was performed at a flow rate of 1.0 mL/min. A representative chromatogram of 21 NBD-amino acids under gradient elution was shown in Figure 4-3 (a). The analysis could be completed in 7 min. The analysis time was shortened in comparison with our previous methods using the monolithic silica column [62, 64].

4.3.4 Analytical method validation

As listed in Table 4-2, the limits of detection for all the NBD-amino acids ranged from 1.2 to 23.3 nM at a signal-to-noise ratio of 3, and the limits of quantitation were in the range from 4.1 to 77 nM at a signal-to-noise ratio of 10. The linearity in the range from 0.02 to 20 μM was examined. The peak height ratios of the analytes to the internal standard versus the injection amounts were plotted, and linear regressions were calculated. The correction coefficients for all the NBD-amino acids were better than 0.999.

The data of the intra-day precision, the inter-day precision, and the accuracy were showed in Table 4-2. The intra-day and inter-day precisions were determined by analyzing the plasma sample five times in one day and five times over five consecutive days, respectively. The intra-day precisions were from 1.3 to 4.1%, and the inter-day precisions were in the range from 1.1 to 5.3 %. Standard amino acid solutions of different concentrations (0, 2, 4, and 6 μM) were added to the mouse plasma sample to assess the accuracy of the method. Then, calibration curves could be obtained by the same method as described before. The ratios of the slopes of the standards-spiked plasma samples to the standard amino acids were calculated for the accuracies. The accuracies for all the NBD-amino acids were ranging from 90.9 to 107%. The results showed that the present method was reliable for the analysis of amino acids in the mouse plasma sample.

4.3.5 Application to mouse plasma samples

The developed method was applied to determine the amino acids in a mouse plasma sample to investigate the suitability of the method for the analysis of biological samples. Figure 4-3 (b) shows the chromatogram obtained from mouse plasma sample, and the amino acid concentrations are presented in Table 4-3. The concentrations corresponded to the values that were obtained in our previous research [62, 64]. The concentrations of Aspartic acid and cystine, which could not be determined by using a 250-mm-long monolithic silica column, could be analyzed by the developed method. According to the obtained data, Gln was found to be the most abundant amino acid [65], with concentrations reaching 537.6 μM, while the concentration of cystine was only 2.9 μM. Even if there were big concentration differences among the different amino acids, all can be quantified with high accuracy. The results showed that the present method can be applied to monitor the concentrations of amino acids in biological samples.

4.4 Conclusions

The analysis of 21 NBD-amino acids was successfully performed on a core-shell particle column within 7 min, which was much faster comparing with conventional particle-packed column [46] and monolithic silica column (Chapter 3). From the investigation of the chromatographic properties, the minimum theoretical plate height of the core-shell particle column reached 5.1 μm, which was only half of the values obtained by the conventional particle-packed column and monolithic silica column. It was observed that there was no significant effect on the separation efficiency after increasing the flow rate. The determination of amino acids in mouse plasma sample was also carried out with this method. It was proven to be fast, accurate, and precise, and was applicable to the analysis of amino acids in biological samples. This method can be a potential tool to clarify the physiological roles of amino acids in biological activity and the diagnosis of disease.

Figures

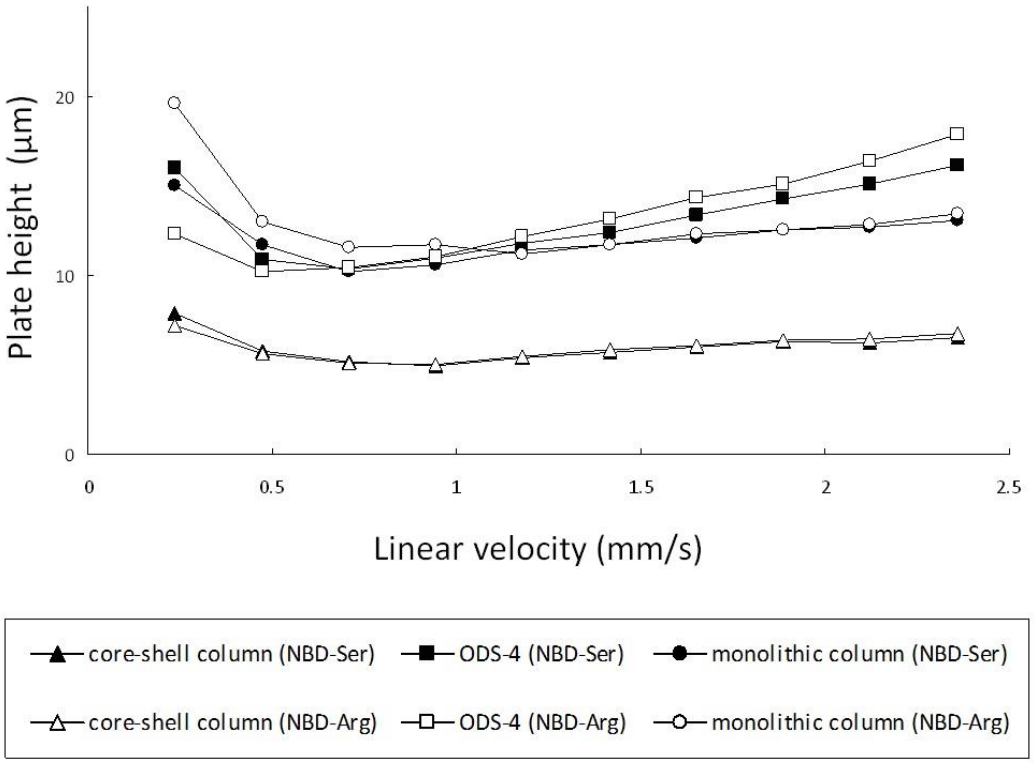

Figure 4-1. van Deemter plotting for NBD-Ser and NBD-Arg using a conventional particle-packed column (ODS-4 column), a monolithic silica column (MonoClad C18-HS), and a core-shell particle column (Kinetex C18-100A)

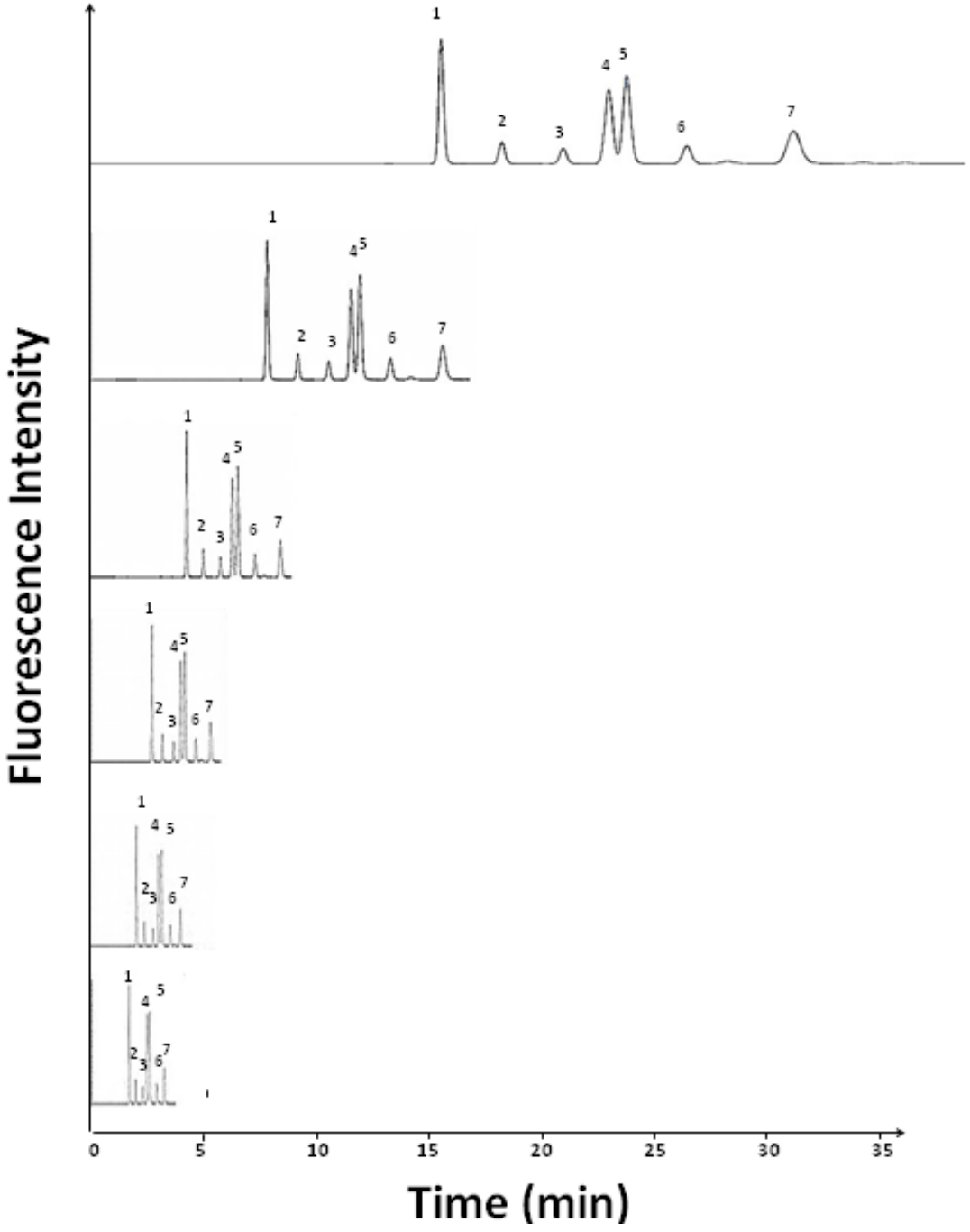

Figure 4-2. Chromatogram of 7 NBD-amino acids obtained at the flow rates of 0.1, 0.2, 0.4, 0.6, 0.8, and 1.0 mL/min.

Peaks in the chromatogram: 1, NBD-histidine; 2, NBD-asparagine; 3, NBD-glutamine; 4, NBD-serine; 5, NBD-arginine; 6, NBD-citrulline; and 7, NBD-OH.

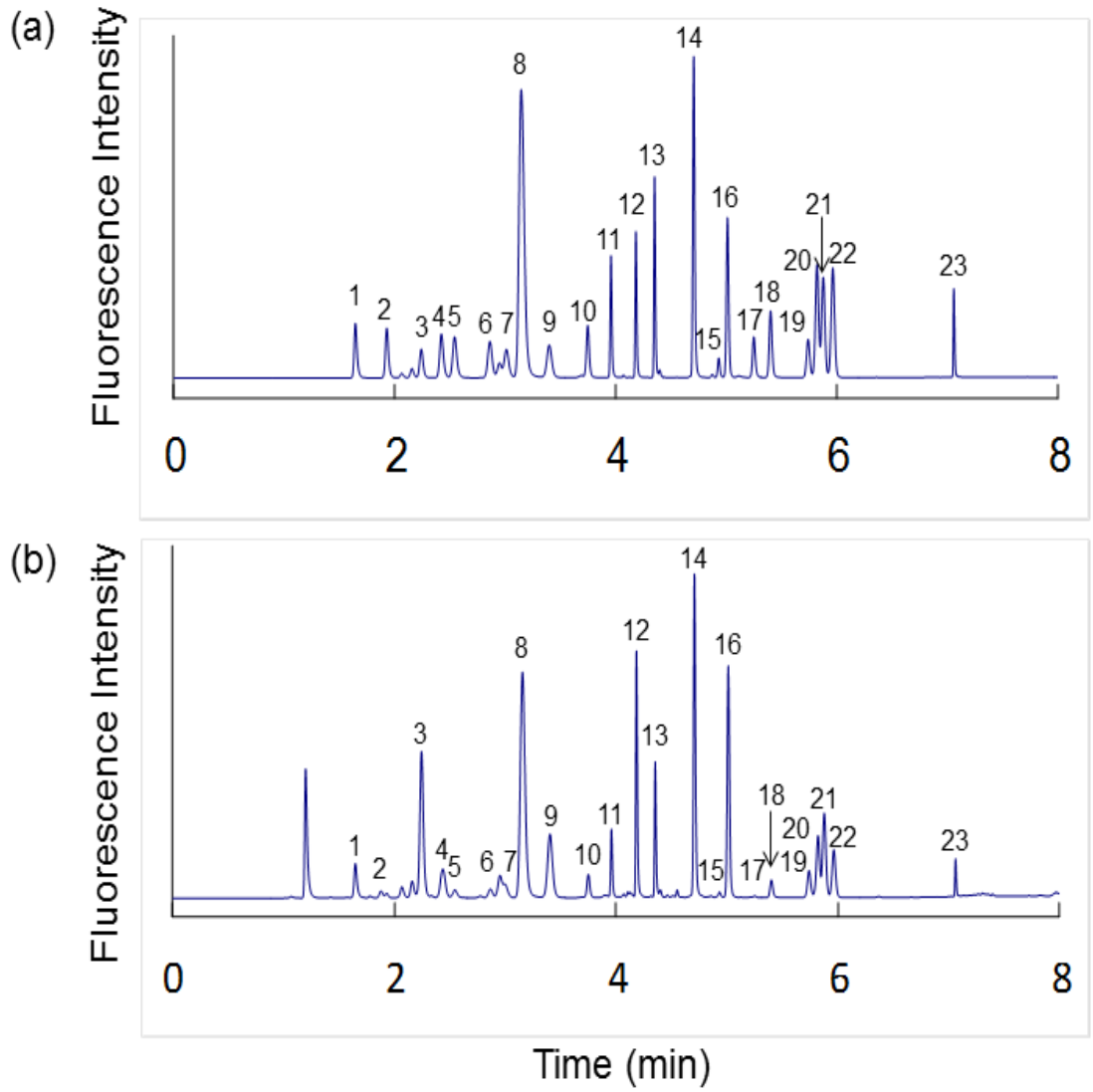

Figure 4-3. Chromatograms of (a) 21 NBD-amino acid solution and (b) a derivatized mouse plasma sample.

Peaks in the chromatogram: 1, NBD-histidine; 2, NBD-asparagine; 3, NBD-glutamine; 4, NBD-serine; 5, NBD-arginine; 6, NBD-citrulline; 7, NBD-aspartic acid; 8, NBD-OH; 9, NBD-glycine; 10, NBD-glutamic acid; 11, NBD-threonine; 12, NBD-alanine; 13, NBD-proline; 14, NBD-6-aminocaproic acid (internal standard); 15, NBD-methionine; 16, NBD-valine; 17, NBD-cystine; 18, NBD-ornithine; 19, NBD-lysine; 20, NBD-isoleucine; 21, NBD-leucine; 22, NBD-phenylalanine; and 23, NBD-tyrosine.

Tables

Table 4-1. Chromatographic parameters obtained at different flow rates

Flow rate (mL/min)	Rs (NBD-Ser and NBD-Arg)	Retention time of NBD-Arg (min)	Column pressure (MPa)	Theoretical plate height (NBD-Arg, μm)	Theoretical plate number (NBD- Arg)
0.1	1.20	23.6	4.7	7.1	21000
0.2	1.33	11.7	9.4	5.8	26000
0.3	1.53	7.9	14.2	5.3	28000
0.4	1.61	6.0	18.8	5.3	28000
0.5	1.58	4.8	23.4	6.0	25000
0.6	1.58	4.1	28.0	6.4	23000
0.7	1.59	3.5	32.5	7.0	21000
0.8	1.56	3.1	37.1	7.5	20000
0.9	1.62	2.8	41.5	7.5	20000
1.0	1.61	2.5	46.0	8.0	19000

Table 4-2. Validation data of the proposed method for the determination of mouse plasma

Amino acid	Limits of detection (nM)	Limits of quantitation (nM)	Intra-day precision (%) (n=5)	Inter-day precision (%) (n=5)	Accuracy (%)(n=3)
His	4.8	15.8	1.9	1.6	107±2.9
Asn	11.8	39.4	2.6	2.5	92.0±3.8
Gln	18.5	61.5	3.9	2.9	95.3±4.0
Ser	1.9	6.2	2.4	2.5	104±11
Arg	4.9	16.2	3.9	2.4	97.8±8.7
Cit	23.3	77	2.1	2.8	97.0±5.6
Asp	7.8	25.8	2.2	2.8	99.9±6.4
Gly	3.0	10.0	2.2	1.6	107±3.1
Glu	10.5	34.8	1.6	2.7	102±11
Thr	2.9	9.6	3.5	1.2	105±9.1
Ala	1.2	4.1	2.5	5.3	101±4.6
Pro	2.0	11.6	2.4	2.6	103±4.2
Met	8.9	29.7	3.7	1.9	98.7±11.6
Val	3.0	10.2	2.6	2.9	97.5±15.6
Cystine	12.1	38.7	2.8	1.8	90.9±3.0
Orn	5.7	18.8	3.7	2.9	95.1±6.5
Lys	6.0	19.9	3.8	1.2	92.9±6.2
Ile	5.4	17.9	3.9	2.5	101±13
Leu	7.2	23.8	2.5	1.1	102±14
Phe	5.6	18.5	1.3	2.5	106±6.4
Tyr	4.6	15.2	4.1	4.2	94.9±11.7

Table 4-3. Concentrations of amino acids in mouse plasma sample

Amino acid	Concentrations in mouse plasma sample (μM)	Amino acid	Concentrations in mouse plasma sample (μM)
His	52.4	Pro	60.3
Asn	12.4	Met	42.5
Gln	538	Val	151
Ser	101	Cystine	2.9
Arg	23.8	Orn	37.4
Cit	23.7	Lys	85.8
Asp	21.5	Ile	56.6
Gly	201	Leu	92.3
Glu	55.8	Phe	44.3
Thr	69.3	Tyr	62.8
Ala	207		

Chapter 5. Fast and quantitative analysis of branched-chain amino acids in biological samples using pillar array column

5.1. Introduction

Branched-chain amino acids (BCAAs) are a group of essential amino acids that have aliphatic side-chains with a branch (a carbon atom bound to more than two other carbon atoms). Among proteinogenic amino acids, there are three BCAAs: leucine (Leu), isoleucine (Ile), and valine (Val) (Figure 5-1). With the mechanism that BCAAs regulate gene expression at the level of mRNA translations, BCAAs could modulate protein synthesis in physiological important tissues through both of the insulin- and mammalian target of rapamycin (mTOR)-independent signaling pathway [66]. Besides, valine supports neurotransmitter glutamate synthesis during synaptic activity [67]. In adipose and muscle tissue, leucine is used in the formation of sterols [68]. Isoleucine participates in the synthesis of ketone bodies or fatty acids [69]. Recently, BCAAs have been found to be closely related to diseases (Table 5-1). Therefore, the analysis of BCAAs has been attracting great research interests [70-74]. In Chapter 3 & 4, the analyses of NBD-amino acids including BCAAs were developed by using monolithic silica column and core-shell particle column, respectively. The analysis time has been shortened to 7 min [75]. However, it is needed to fasten the analysis as to meet the clinical diagnosis requirement. In my gourp's previous study, six fluorescently labeled amino acids were successfully separated in 140 s by pillar array column [32]. However, to date, pillar array column have not been used for quantitative analysis. In this study, pillar array column was used for the fast analysis and quantification of BCAAs in sports drink and plasma samples.

5.2 Experimental section

5.2.1 Chip fabrication

The microchips were fabricated by ultraviolet (UV) photolithography and deep reactive ion etching (DRIE). First, a 270-nm thick silicon oxide layer was fabricated on a 20 × 20 × 0.2 mm silicon substrate by thermal oxidation at 1000 °C. The holes pattern for the inlets and the outlets were defined by UV photolithography (MA-6, SUSS MicroTec, Germany). The underlying silicon oxide layer was wet-etched by buffered hydrofluoric acid to fabricate the holes pattern. The pillar array and an injection channel were patterned by UV photolithography and wet-etching. After the exposed silicon oxide layer was wet-etched, the silicon layer was dry-etched by DRIE (Multiplex-ICP, Sumitomo Precision Products, Hyogo, Japan) to fabricate a 30 μm deep injection channel and through holes. Another 30 μm deep channel was dry-etched on the silicon layer by DRIE to form the pillar array channel, the injection channel, and flow through holes. The depth of the pillar channel was 30 μm and the total depth of the injection channel was 60 μm. The pillars in the separation channel were 3-μm squares, each with an interpillar distance of 2 μm. After the oxide layer was wet-etched, the surface of the micro-channel was oxygenated using oxygen plasma (RIE-10NR, Samco, Kyoto, Japan) for subsequent surface modification. Finally, the silicon substrate was bonded to a Pyrex glass plate (Corning 7740, Corning Inc., New York, NY) by anodic bonding (NEC Corporation, Tokyo, Japan). After fabrication of the microchip, dimethyloctadecylchlorosilane was used to modify the surface of the separation channel for reversed-phase separation.

In this study, low-dispersion turns were used for folding the pillar array column in a microchip (Figure 5-2). The column length was 110 mm. The widths of channels in the straight part and the turns were 400 and 110 μm, respectively. The total external porosity ε was approximately 0.6.

5.2.2 Fluorescence derivatization of branched-chain amino acids

Twenty microliters of a solution of BCAAs and 20 µL of an internal standard solution (0.1 mM 6-aminocaproic acid) were added to 180 µL of 0.2 M borate buffer solution (pH 9.0). Then, 40 µL of 10 mM NBD-F were added and the mixture was heated in a water bath at a temperature of 60 °C for 5 min. After cooling the reaction mixture in ice water, 740 µL of 50 mM HCl solution were added to the reaction mixture. The resultant solution was injected into the microchip LC system.

5.2.3 Pretreatment of sports drink sample

Twenty microliters of drink sample were diluted with 1980 µL of 50 mM HCl. The diluted sample was fluorescently derivatized as described above.

5.2.4 Pretreatment of human plasma sample

In order to remove proteins in the plasma sample, 600 µL of methanol and 600 µL of acetonitrile were added to 200 µL of plasma sample. Then the sample was centrifuged at 10 000 *g* for 40 min. The supernatant was evaporated to dryness under reduced pressure at room temperature. The residue was derivatized with NBD-F as described above.

5.2.5 Chromatographic conditions

A water–acetonitrile–TFA (92:8:0.02, v/v/v) mixture was used as the mobile phase. The mobile phase was pumped into the microchip using a micro-HPLC pump (MP711, GL Sciences, Tokyo, Japan). The flow rate was set at 2 µL/min. An IX70 inverted microscope system (Olympus, Tokyo, Japan) was used for determination of the fluorescence intensity. In this system, a UPlanApo 20× (N.A. 0.70, Olympus) objective and an electron-multiplying charge-coupled device camera (iXon3, Andor

Technologies, South Windsor, CT, USA) were mounted for observation of the separation channel and fluorescence band. Fluorescence excitation was performed using a metal halide lamp. The filter cube had a BP460-490 excitation filter (Olympus), a 505DRLP dichroic mirror (Omega Optical, Brattleboro, VT, USA), and an HQ 535m emission filter (Chroma Technology, Rockingham, VT, USA). A PSL-3F slit (Sigma Koki, Tokyo, Japan) was placed between the emission filter and the photocounter tube for confinement of the detection area. The detection point was set near the outlet of the pillar array column. The fluorescence intensity was analyzed using an H7421-40 photomultiplier tube equipped with a PHC-2500 photocounter. The sample was injected into the pillar array column using a four-port valve (Valco Instruments, Houston, TX, USA) and a commercially available syringe (Hamilton, Reno, NV, USA).

5.2.6 Validation study

Standard stock solutions were prepared by dissolving amino acids in 100 mM HCl solution. Solutions with different concentrations of amino acids (20, 40, 100, 200, and 1000 μM) were prepared from the stock solutions. Linear calibration curves were produced by plotting the ratios of the peak heights of the NBD-amino acids to the internal standard versus the injection amounts of the NBD-amino acids. Intra- and interday precision experiments were performed by analyzing the plasma samples five times in the same day and once per day for five consecutive days, respectively. To evaluate the accuracy of the analytical method, standard amino acids of different concentrations (200, 400, and 600 μM) were added to a human plasma sample. The accuracy was calculated by dividing the value of the slope obtained from the standard-spiked plasma sample by that of the slope for the standard amino acids.

5.2.7 Analysis of branched-chain amino acids using conventional LC system

The analysis of BCAAs using conventional LC was based on our previous research

[64].

5.3 Results and discussion

5.3.1 Optimization of chromatographic conditions

In my previous study [32], water–acetonitrile–TFA (90:10:0.02, v/v/v) was used as the mobile phase for the separation of six NBD-amino acids (proline (Pro), Val, 6-aminocaproic acid, Ile, Leu, and phenylalanine (Phe)). The analysis time was about 140 s. Besides, a microscope system was applied for on-chip detection of fluorescence intensity (Figure 5-3). In contrast to off-chip detection, the on-chip detection was devoid of after-column volume which could contribute to the band broadening [31, 76].

In order to achieve a faster analysis of only BCAAs, the chromatographic conditions, including flow rate, the detection point on the chip, and composition of the mobile phase, were investigated.

First, considering the fast analysis and pressure limitations of microchip, the experiments were performed at the flow rate of 2 μL/min. In my group's previous paper [32], mobile phase of water–acetonitrile–TFA (90:10:0.02, v/v/v) was used as the mobile phase and it was eluted at the flow rate of 0.5 μL/min. However, when the flow rate was increased to 2 μL/min, the separation of NBD-Val and NBD-6-aminocaproic acid was overlapped. Then the effect of detection point was examined. From the Figure 5-4, it can be seen that the NBD-Val and NBD-6-aminocaproic acid obtained a better separation with a longer pillar array column. Therefore, detection point was set near the outlet of the pillar array column.

Lacing in good separation of NBD-Val and NBD-6-aminocaproic acid, the composition of the mobile phase was investigated in the following study. Separation was performed by using three different mobile phases (water–acetonitrile–TFA

(90:10:0.02, 92:8:0.02, and 95:5:0.02)). As shown in the Figure 5-5, it was observed that NBD-Val and NBD-6-aminocaproic acid could obtain a better separation with a lower concentration of acetonitrile in the mobile phase, while NBD-Ile and NBD-Leu was separated well with a higher concentration of acetonitrile. Therefore, water–acetonitrile–TFA (92:8:0.02, v/v/v) was selected as the mobile phase.

A representative chromatogram of NBD-BCAAs is shown in Figure 5-6(a). The separation was achieved within approximately 100 s, which was about two-thirds of the time taken in my previous study [32]. The sample was injected for 5 times consecutively for calculation of the reproducibility of the retention time of the three NBD-BCAAs. The reproducibilities for NBD-Val, NBD-Ile, and NBD-Leu were 2.57, 2.82 and 2.58 %, respectively, which ensured a valid analysis.

5.3.2 Linearity, limits of detection, and limits of quantification

First, the reproducibility of the peak intensity detected on the photomultiplier tube was investigated. However, the injection amount was approximately 1 nL, which was too small to be controlled. The relative standard deviation of the peak intensity was 28.4 % when NBD-Val was injected at a concentration of 2 μM. In order to elimination of the effects of uncontrollable injection amount and improve precise of quantitative analysis, 6-aminocaproic acid as an internal standard was added, and the ratio of the peak intensity of NBD-Val to that of the internal standard was calculated. The addition of an internal standard improved the reproducibility to 3.23 %. Similar results were also achieved for the other NBD-BCAAs. These results show that the reproducibilities for all NBD-BCAAs were improved with the help of an internal standard, and quantitative analysis of BCAAs can be performed using a pillar array column.

The calibration curve for each NBD-BCAA showed good linearity in the range 0.4 to 20 μM. The limits of detection (LODs) and limits of quantification (LOQs) for the NBD-BCAAs were each calculated as the concentration and the injection amount. For comparison, the values obtained with conventional LC in Chapter 3 were used. As

shown in Table 5-2, when the LODs and LOQs for individual NBD-amino acids were calculated as the concentrations at signal-to-noise ratios of 3 and 10, respectively, the values obtained using the pillar array column were significantly higher than those obtained using conventional LC. However, when the LODs and LOQs were calculated as injection amounts, the values obtained using the pillar array column were comparatively lower than those obtained using conventional LC. This was clearly due to the difference between the injection amounts in these two methods. When conventional LC was used, the injection amount was 10 μL, whereas the injection volume was only about 1 nL in the microchip LC system. In order to improve the sensitivity, more studies are necessary. A blue laser, which matches the excitation wavelength of the NBD-BCAAs, might be useful for fluorescence irradiation to obtain a stronger signal [77]. As there are pillar arrays at the detection area in this study, the design of the detection area on the microchip needs to be optimized. On-chip sample preconcentration before separation with the pillar array column might increase the detection sensitivity and simplify sample pretreatment [78].

5.3.3 Determination of branched-chain amino acids in sports drink sample

Some research has revealed that an intake of BCAAs can delay the production of lactic acid and lead to maintenance of endurance exercise capacity [79]. Besides, BCAAs, particularly leucine, have anabolic effects on protein metabolism by increasing the rate of protein synthesis and decreasing the rate of protein degradation in human muscle during recovery from endurance exercise [80, 81]. Therefore, BCAAs are often used in the sports drink. The developed method was used to determine BCAAs in a sports drink; the BCAA concentration has to be sufficiently high to serve as a good example for the first application of the method to real samples. After dilution and derivatization with NBD-F, the sample was analyzed using pillar array columns. The chromatogram obtained from the sports drink sample is shown in

Figure 5-6(b). The peaks of the NBD-BCAAs and NBD-6-aminocaproic acid were well separated. There were no other peaks interfering with the analysis of the NBD-BCAAs. The sports drink also contains arginine, but because arginine is hydrophilic, NBD-arginine was easily eluted and overlapped with the peak of NBD-OH. Precision and accuracy data are listed in Table 5-3. These results showed that the method was valid for the determination of BCAAs in a sports drink. The concentrations of amino acids determined using pillar array column and conventional LC are presented in Table 5-4. These values showed good agreement with the concentrations reported in the product brochure.

5.3.4 Determination of branched-chain amino acids in human plasma sample

The developed method was applied to a human plasma sample. This is more difficult because the plasma sample has many other endogenous compounds. In addition, the concentrations of BCAAs are much lower than in a sports drink. The chromatogram obtained from the human plasma sample is shown in Figure 5-6(c). Because most of the NBD-amino acids were very hydrophilic, they were easily eluted and overlapped with the NBD-OH peak when the optimized mobile phase was used. Precision and accuracy experiments were carried out to evaluate whether the developed method could be useful for routine analysis of BCAAs in human plasma samples. As shown in Table 5-5, both the intra- and interday precisions (n = 5) were below 5%. The accuracies for the three BCAAs were about 90%. The results indicate that the developed method using the pillar array column is applicable to biological samples. The concentrations of amino acids determined using the developed method and conventional LC are presented in Table 5-6. From the table, it can be concluded that the concentrations obtained using the pillar array column were similar to the data obtained using conventional LC.

5.4 Conclusions

A 110-mm pillar array column, which was folded with low-dispersion turns, was used for fast analysis of BCAAs. The analysis time of fluorescently labeled BCAAs was about 100 s, which was much faster than in previous studies. For quantitative determinations of BCAAs in sports drink and human plasma samples, fluorescence microscopy was used for sensitive detection. With the assistance of an internal standard, the concentrations of BCAAs in these samples were quantitatively determined. The concentrations determined using the developed method showed high agreement with data obtained using conventional LC. The developed method is proved to be useful for clinical diagnosis. Although the sensitivity still needs to be improved, the method using pillar array columns can be used for fast analysis of biological compounds in biosamples such as plasma, urine, and tissue.

Figures

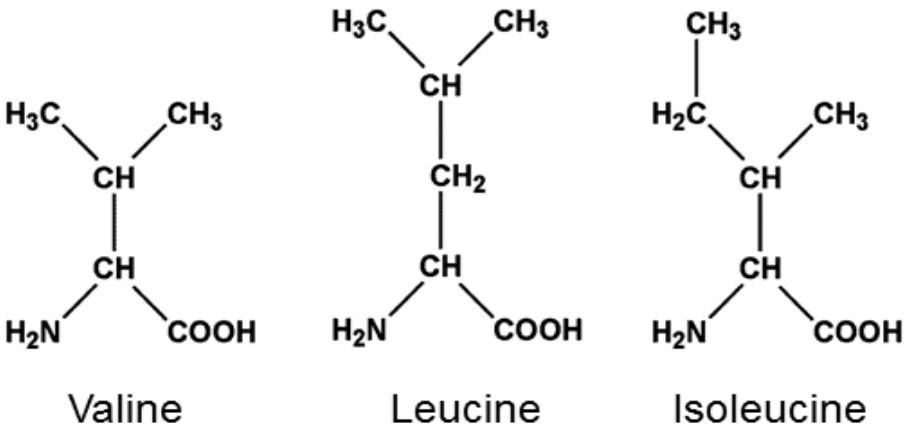

Figure 5-1. Chemical structures of valine, leucine, and isoleucine

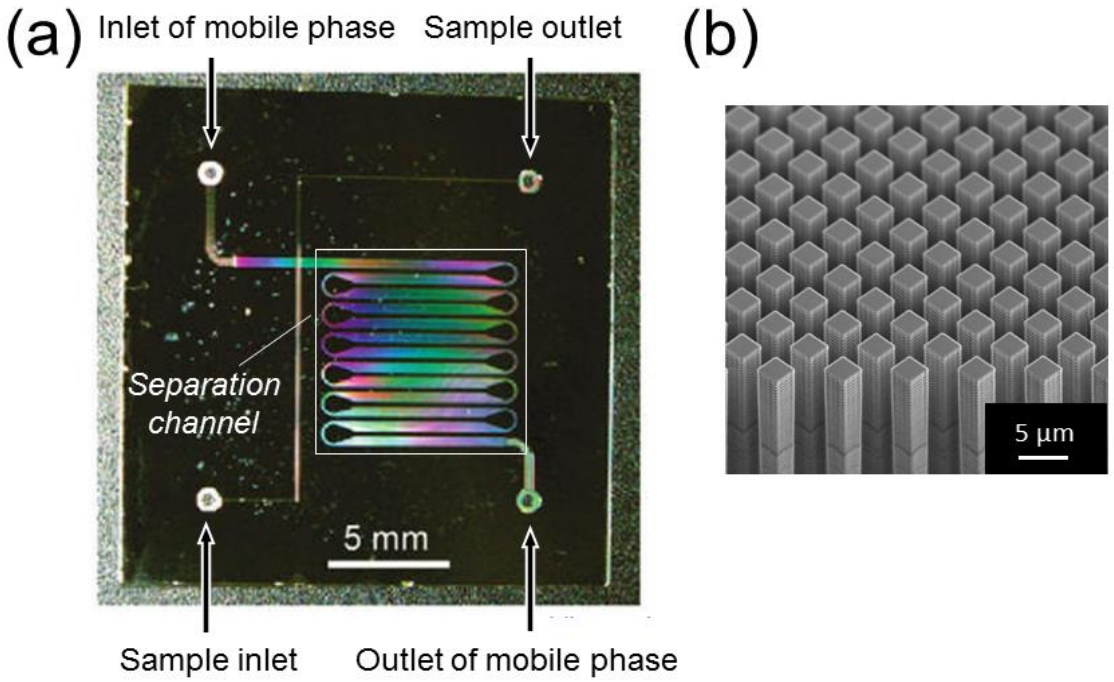

Figure 5-2. (a) Photograph of the fabricated microchip, and (b) scanning electron microscopy image of the pillar array structure

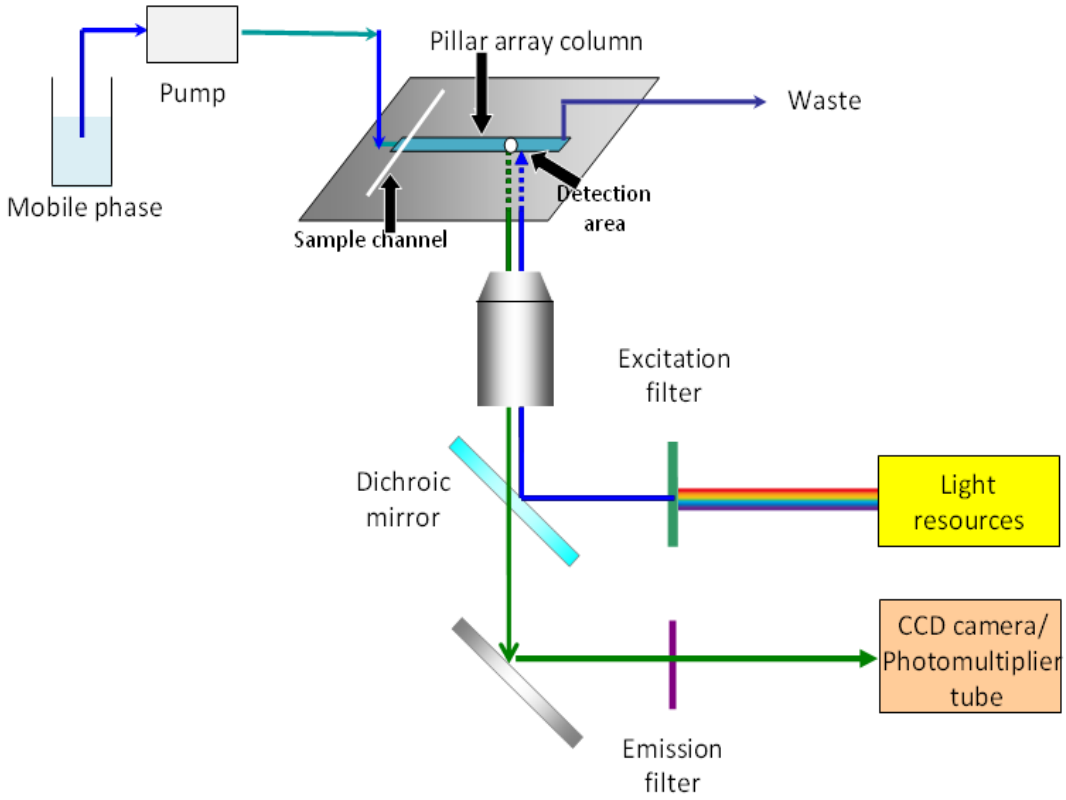

Figure 5-3. The scheme of the chip-LC system and fluorescence microscopy detection system

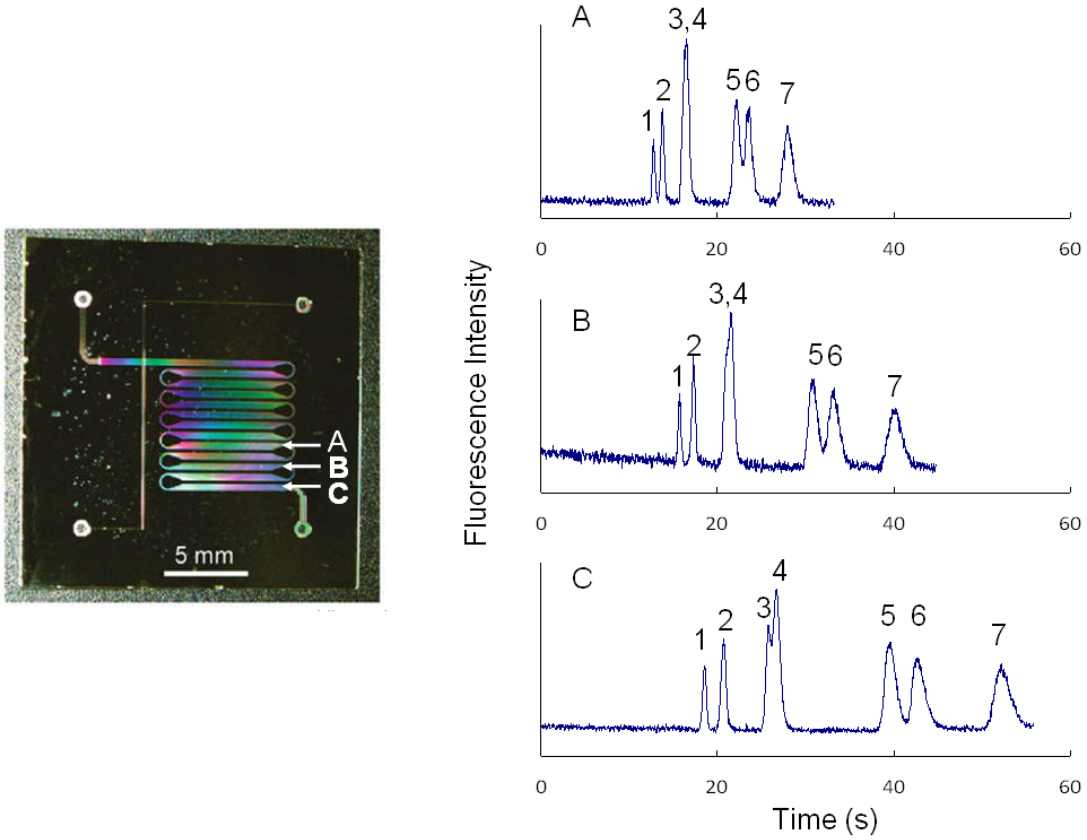

Figure 5-4. Chromatograms obtained from fluorescently labeled amino acid solution on the microchip with low-dispersion turns. Detection was carried out at points (A) 76 mm, (B) 93 mm, and (C) 110 mm downstream of the injection zone. Peaks: 1, NBD-OH; 2, NBD-Pro; 3, NBD-Val; 4, NBD-6-aminocaproic acid; 5, NBD-Ile; 6, NBD-Leu; 7, NBD-Phe.

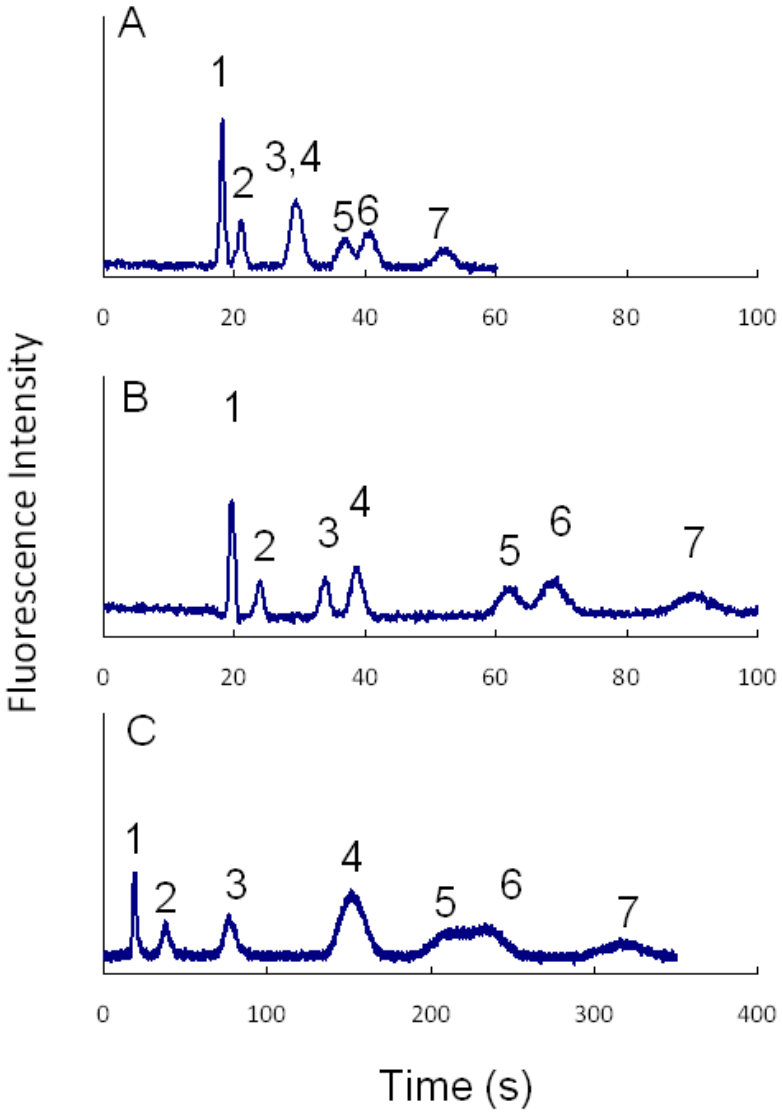

Figure 5-5. Chromatograms obtained by using different mobile phase. (A) water–acetonitrile–TFA (90:10:0.02, v/v/v); (B) water–acetonitrile–TFA (92:8:0.02, v/v/v); (C) water–acetonitrile–TFA (95:5:0.02, v/v/v).

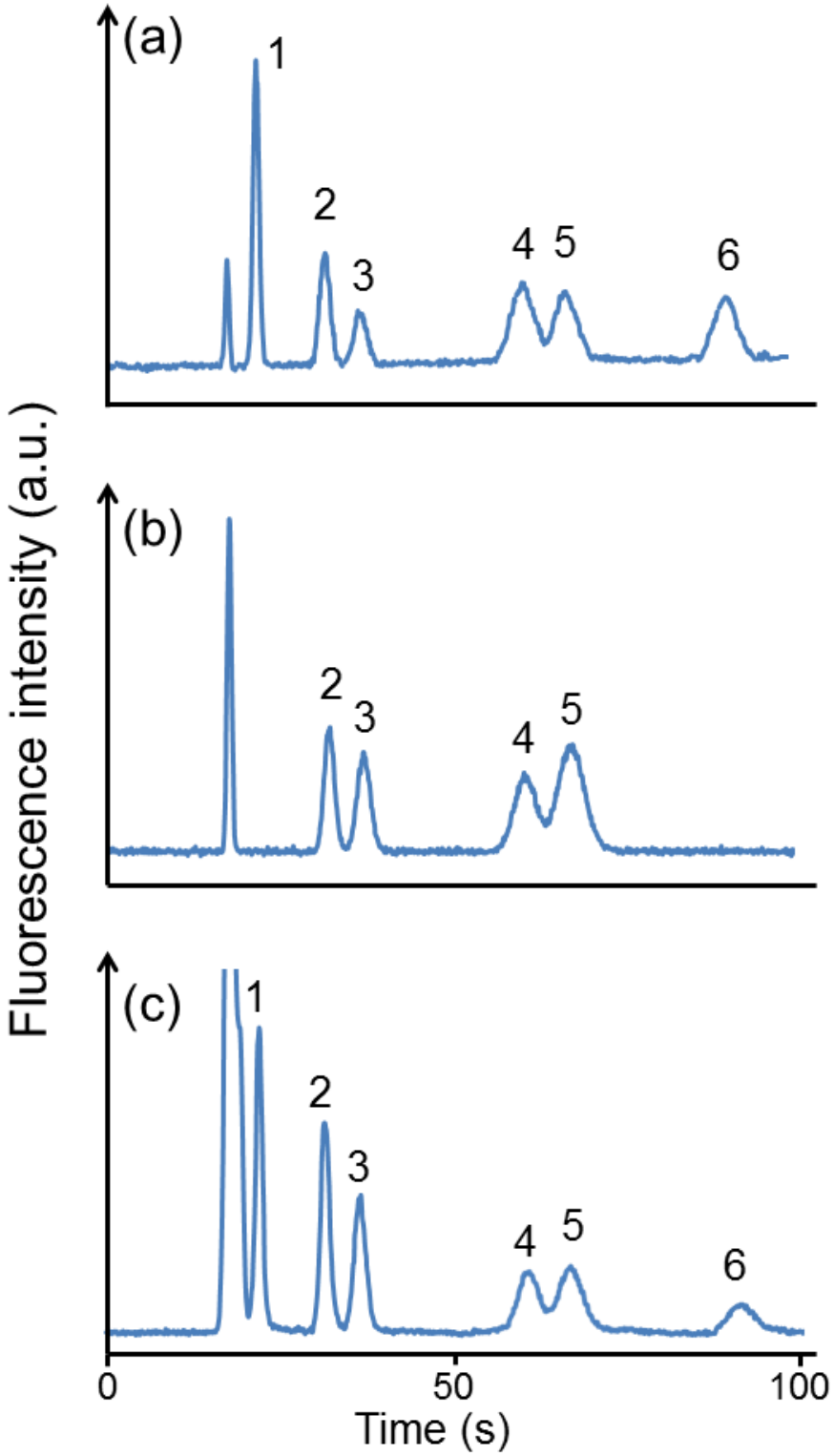

Figure 5-6. Chromatograms of (a) NBD-amino acids solution, (b) sports drink, and (c) human plasma sample. Chromatogram peaks: 1, NBD-Pro; 2, NBD-Val; 3, NBD-6-aminocaproic acid; 4, NBD-Ile; 5, NBD-Leu; and 6, NBD-Phe

Tables

Table 5-1. The relationship between the BCAAs and the diseases

Disease	The concentration change in the biofluids	References
Maple syrup urine disease (MSUD)	↑	[73, 82, 83]
Chronic liver disease	↓	[84, 85]
Heart disease	↑	[86]
Chronic obstructive pulmonary disease	↓	[87]
Huntington disease	↓	[36]
Diabetes	↑	[35, 88, 89]
Obesity	↑	[90]

Table 5-2 Limits of detection and limits of quantification for NBD-BCAAs

Amino acids	LOD (nM)	LOD (fmol)	LOQ (nM)	LOQ (fmol)
Pro	89.3	0.11	298	0.36
Val	107	0.13	355	0.43
Ile	130	0.16	434	0.52
Leu	123	0.15	412	0.49
Phe	161	0.19	538	0.65

Table 5-3. Precision and accuracy of proposed method for determination of BCAAs in sports drink

Amino acid	Intra-day precision (%) (n = 5)	Inter-day precision (%) (n = 5)	Accuracy (%)
Val	2.69	6.97	99.1 ± 1.9
Ile	1.42	4.64	96.9 ± 1.2
Leu	3.03	3.80	90.2 ± 2.4

Table 5-4. Concentrations of BCAAs in sports drink

Amino acid	Concentration reported in product brochure (mg/100 mL)	Concentration determined using pillar array column (mg/100 mL)	Concentration determined using conventional LC (mg/100 mL)
Val	200	188 ± 3.5	200 ± 3.4
Ile	200	214 ± 2.6	200 ± 6.6
Leu	400	392 ± 10	409 ± 13

Table 5-5. Precision and accuracy of developed method for determination of BCAAs in human plasma sample

Amino acid	Intra-day precision (%) (n = 5)	Inter-day precision (%) (n = 5)	Accuracy (%)
Val	1.93	2.74	91.6 ± 1.0
Ile	3.80	3.63	92.6 ± 1.1
Leu	3.19	4.86	92.1 ± 0.8

Table 5-6. Concentrations of BCAAs in human plasma sample

Amino acid	Concentration determined using pillar array column (μM)	Concentration determined using monolithic column (μM)
Val	191 ± 4.0	195 ± 5.5
Ile	72.7 ± 1.6	77.0 ± 3.5
Leu	111 ± 1.5	121 ± 7.8

Chapter 6. Integration of a gradient elution system in a pillar array column for the fast separation of biological compounds

6.1 Introduction

In Chapter 5, fast and quantitative analysis of BCAAs in biological samples were conducted by using pillar array column. However, the developed method under isocratic elution is very difficult to apply the developed method to analyze biological samples, because the compounds in biological samples are very complex and they exhibit large differences in their individual polarity. In conventional LC, this problem is solved by utilizing a gradient elution system that can accelerate the elution of strongly retained solutes. Hence, the development of a gradient elution system with pillar array columns is crucial to shortening the analysis time and being able to perform more effective analyses. The essential component of the gradient elution system is a mixer, which is used to mix two kinds of mobile phases. At present, a micropump that contains a mixer is commercially available [91]. However, after the mobile phases are mixed using this apparatus, they have to be introduced from the mixer into the separation channel, which results in a considerable delay from the time when the gradient program starts. A useful way to eliminate the delay is to setup a direct connection between the mixer and the separation channel. Therefore, in this study, a gradient elution system and a separation channel were integrated on a silicon chip.

In order to make a necessary change in the mobile phase composition during a gradient elution, a micromixer which could conduct a thorough and rapid mixing is necessary, however, mixing two liquid samples in a microfabricated chip is still challenging. Many scientists have attempted to design an effective mixing structure for use on microfabricated chips [92-94]. The recent development of micromixers on

chips can be divided into two categories: active mixers and passive mixers [95]. Active mixers apply external energy force, including magnetic stirring devices, acounstic, and use gas bubbles, to mix two fluids [96, 97]. However, it is generally more complex, and is difficult to operate, fabricate, and integrate them on to chips that contain other microfluidic components. Hence, more attention is now being focused on the development of passive mixers, in which the mixing process is relying entirely on the modified microchannel with different shapes or structures. The mixing is enhanced by the increased contact area and contact time of the two fluids. Compared with active mixers, the passive mixers have the advantages of low cost, ease of fabrication and operation, and can be integrated into microfluidic systems [98, 99]. Based on a computational fluid dynamics (CFD) study, it was found that the cross-Tesla mixer makes more than 90% mixing efficiency attainable. Therefore, I fabricated a cross-Tesla mixer and a separation channel on a silicon chip and performed pressure-driven reversed-phase LC separation using gradient elution.

6.2 Experimental section

6.2.1 Conditions for CFD analysis

In this research, the mixing efficiency of different types of mixing structures and junction part (T-straight, T-Tesla, cross-straight, and cross-Tesla) were investigated. The mixing of water and ethanol was simulated by using commercial computational fluidic dynamic (CFD) software (Coventor-Ware, Coventor, Cary, NC). During the simulation, the diffusion coefficient of water and ethanol was set as 1.2×10^{-9} m^2/s. The flow ratio of water and ethanol was 65:35, and the total flow rate was 1 μL/min. The width and depth of microchannel were set as 100 and 30 μm, respectively.

6.2.2 Conditions for fluid experiments

The T-Tesla and cross-Tesla mixers were fabricated on the microchips, respectively,

and investigated for the mixing of two solutions (water and fluorescein in methanol) at various downstream positions (0, 1, 2, and 3 mm). The total flow rate was set as 1 μL/min. The ratio of water to fluorescein in methanol was 65:35. The fluorescence images of mixing at various positions in the mixers were observed using a fluorescence microscope (IX71, Olympus, Tokyo, Japan). The mixing efficiency which was expressed as the standard deviation of the fluorescence intensity distribution in each micromixer was calculated based on the following equation, $\sigma = \langle (I - \langle I \rangle)^2 \rangle^{1/2}$. In this equation, I is the fluorescence intensity of a pixel, and $\langle\rangle$ indicates an average over all of the pixels in the micromixers. The fluorescence intensities were calculated by utilizing Image J software (National Institutes of Health, Bethesda, Maryland).

6.2.3 Microchip fabrication

The fabrication method is the same as described in section 5.2.1 of Chapter 5.

6.2.4 Evaluation of mixing efficiency of microchip with pillar arrays

The mobile phases were pumped into the pillar array column by using a micro-HPLC pump, MP711 (GL Sciences, Tokyo, Japan), which has two branch pumps. With the help of the two branch pumps, two kinds of mobile phases could be eluted on the microchip at different flow rates. Each sample was injected into the microchip by using a commercially available syringe and a four-port valve (Valco Instruments, Houston, TX).

To investigate the mixing efficiency of the mixer in the microchip, two fluids (water and fluorescein in methanol) were pumped into the microchip of the mobile phase at constant flow rates from two inlets. The ratios of the flow rates of the two liquids were 9:1, 7:3, 5:5, 3:7, and 1:9. Under the gradient elution condition, water was eluted isocratically in the first 30 s, and the percentage of fluorescein in methanol increased from 0 to 100 % in the following 60 s. An IX70 inverted microscope

(Olympus, Tokyo, Japan) was used to observe the fluorescence image of the microchip. Excitation was carried out using a metal halide lamp. The filter cube comprised a BP460-490 excitation filter (Olympus), a 505DRLP dichroic mirror (Omega Optical, Brattleboro, VT), and an HQ 535m emission filter (Chroma Technology, Rockingham, VT). Fluorescence images of the separation channel entrance were captured using an UplanFL 4× (N.A. 0.13, PhL, Olympus) objective or UplanFL 10x (N.A. 0.30, PhL, Olympus) and an ORCA-ER CCD camera (Hamamatsu Photonics, Hamamatsu, Japan). The pixel size that we used was 1.58 μm.

6.2.5 Separation of coumarin dyes

Two coumarin dyes, C525 and C545 (Exciton, Dayton, OH), were separated by both isocratic elution and gradient elution. For isocratic elution, the mobile phase, water/acetonitrile (65/35), was eluted at a flow rate of 2.0 μL/min. For the gradient elution condition, water and acetonitrile were used as the mobile phases. The gradient conditions were 0–120, 0–60, or 0–30 s, 35–100 % acetonitrile, and the flow rate of the mobile phase was set at 2.0 μL/min. An UplanFL 20× (N.A. 0.70, Olympus) was used to observe the sample band, and an H7421-40 photomultiplier tube (Hamamatsu Photonics) equipped with a PHC-2500 photocounter (Scientex, Hamamatsu, Japan) was used to analyze the fluorescence intensity.

6.2.6 Separation of NBD-aliphatic amines

4-Fluoro-7-nitro-2,1,3-benzoxadiazole (NBD-F, Dojindo Laboratories, Kumamoto, Japan) was used to derivatize aliphatic amines. The derivatization procedure was carried out as follows. Twenty microliters of amine solution (0.5 mM each of pentylamine, hexylamine, heptylamine, and octylamine) was added to 200 μL of 0.2 M borate buffer (pH 8.5). Then, NBD-F solution (10 mM in acetonitrile) was added, and the resulting mixture was heated in a water bath (60 °C) for 5 min. After cooling

in ice water, 200 µL of 50 mM HCl solution was added to stop the reaction. For isocratic elution, water/acetonitrile/trifluoroacetic acid (TFA) (90/10/0.1, v/v/v) was used as the mobile phase. The gradient elution condition was as follows: eluent A was water/acetonitrile/TFA (90/10/0.1, v/v/v) and, eluent B was water/acetonitrile/TFA (10/90/0.1, v/v/v). The gradient program was (0 s, 100/0; end, 0/100). The gradient times were 450 s and 90 s. The total flow rate was kept at 1.0 µL/min. Detection was carried out using an H7421-40 photomultiplier tube (Hamamatsu Photonics, Hamamatsu, Japan) with a PHC-2500 photocounter (Scientex, Hamamatsu, Japan).

6.3 Results and discussion

6.3.1 Evaluation of mixers

In order to achieve effective mixing, both the inlet junction component and mixing component of a micromixer were considered. For the junction component, T-shape and cross-shape structures were taken into account. For the mixing component, a Tesla structure was chosen; this structure has been used elsewhere as a passive microfluidic mixer [98, 99] although its use has not been examined for the mixing of water and organic solvent. For comparison, a straight channel was also examined. CFD analysis was performed, and the results of which are shown in Figure 6-1. In Figure 6-1, the color indicates the percentage of water in the mixed solution (Blue: 0 %; Red: 100 %). When water and ethanol mix well, the color should change to greenish yellow. As shown in Figure 6-1, the color of the microchannel was not so homogeneous after the mixed solutions traveled through T-straight and cross-straight mixers. In a microfluidic system, the Reynolds number (*Re*) is smaller than 100, which indicates that the flow mode in the microchannel is typically laminar. Under this flow mode, the mixing of two solutions is dominated by diffusion, which is quite time-consuming and inefficient. While in the T-Tesla and cross-Tesla mixers, the color of the mixed solutions became yellow-green, and the color indicated that better mixing of two solutions was obtained by applying the Tesla mixers than straight type

mixers. Therefore, the mixing efficiencies of Tesla mixers were investigated in the following experiments.

To confirm the results of the CFD analysis, microchips with a T-Tesla structure or a cross-Tesla structure were fabricated, and their properties were examined. Figure 6-2(a) illustrates the mixing of two fluids (water and fluorescein in methanol) at various downstream positions (0, 1, 2, and 3 mm). From the images, it can be seen that water and fluorescein in methanol were completely mixed at 3 mm downstream from the starting point. The degree of mixing was quantified as the standard deviation of the fluorescence intensity distribution of the microchannel in the images (Figure 6-2(b)). From the Figure 6-2(b), it can be seen that the σ reduced from 0.35 to 0.2 after the mixed solution traveled for 3 mm in the T-Tesla mixer, however, the mixing efficiency could not meet the demand for the fast mixing. In the cross-Tesla mixer, the σ reduced to 0.05, which indicated that more than 90% mixing had occurred. The value σ of the fluorescence intensities at 3 mm downstream of the cross-Tesla structure at different flow rates ranging from 0.5 to 3 μL/min was also investigated. The values are also below 5.0 %, which showed that the flow rate had little influence on the mixing efficiency. Therefore, the cross-Tesla structure was found to be the most efficient at mixing two liquids, and it was applied to the subsequent study.

6.3.2 Mixing efficiency evaluation of microchip with pillar arrays

A cross-Tesla mixer with a length of 18 mm, a separation channel with pillar arrays, and a sample injection channel were fabricated on a microchip as a gradient elution system (Figure 6-3). Even though mixing at 3 mm was highly efficient, the 18-mm-long mixer was fabricated on a chip to bring about complete mixing. The separation channel was 58 mm long and had six low-dispersion turns, which have been found to improve the separation efficiency. In order to confirm that the gradient system worked well, two liquids, water and fluorescein solution in methanol, were pumped into two inlets of the mobile phase at different flow rates under isocratic elution. The ratios of water and the fluorescein solution were 9:1, 7:3, 5:5, 3:7, and

1:9, and the fluorescence intensity in the separation channel was homogeneous in each experiment (Figure 6-4). To confirm the mixing efficiency quantitatively, σ was calculated based on the equation described in the section 6.2.2. The values of σ calculated from each image were less than 4.9%, which indicated that more than 90% mixing efficiency had been achieved. In addition, the fluorescence intensity in the separation channel became greater with the increased ratio of the fluorescein solution. It was also found that there was a linear relationship between the fluorescence intensity and the ratio of the fluorescein solution (Figure 6-5). These results indicated that when the two liquids were pumped under the isocratic elution condition, they were well-mixed upon entering the separation channel.

In order to further examine the mixing efficiency, the two liquids were pumped into each inlet of the mobile phase under the gradient elution condition. Figure 6-6 presents the relationship between the fluorescence intensity in the separation channel and the gradient time. For the first 30 s, water was eluted isocratically as the mobile phase. As seen in Figure 6-6, the fluorescence intensity remained stable for 30 s. Then, the intensity started to increase at 37 s, which indicated that only a 7 s delay existed after the gradient program started. After 37 s, the fluorescence intensity increased gradually with the analysis time, indicating that the two liquids had been mixed efficiently. These experiments proved that the mixer efficiency was high. It should therefore be possible to develop a gradient elution system on a chip using this apparatus.

6.3.3 Separation of coumarin dyes under the gradient elution condition

The chip with a separation channel and mixer was used to separate coumarin dyes, Coumarin 525 and 545, under the gradient elution condition. As shown in Figure 6-7 (a), Coumarin 525 and 545 were separated in 56 s under the isocratic condition with a mobile phase of water/acetonitrile (65/35). Figure 6-7 (b), (c), and (d) show the separation of the two dyes under gradient conditions. The gradient times of the experiments that are presented in Figure 6-7 (b), (c), and (d) were 120, 60, and 30 s,

respectively. Under the gradient elution condition, the retention times for Coumarin 525 and 545 became shorter with the shortening of the gradient time. When the gradient time was 30 s, the two dyes were separated in 30 s, which was only half the time for isocratic elution. Also, the peak shape of Coumarin 545 obtained under the gradient elution condition became sharper compared with the peak shape obtained under the isocratic elution condition. As summarized in Table 6-1, the peak widths of Coumarin 525 and 545 under the gradient elution were smaller than the values obtained under the isocratic elution condition. This shows that gradient elution significantly improves the separation efficiency, which results in increased sensitivity for this type of LC.

6.3.4 Separation of NBD-amines under gradient elution

In order to further investigate the usefulness of a gradient elution system for analyzing biological compounds, aliphatic amines were chosen, because they are involved into many biological reactions, such as the biodegradation of proteins, amino acids, and other biological compounds. Four aliphatic amines derivatized with NBD-F were separated under isocratic and gradient elutions. Figure 6-8 (a) shows the separation of NBD-amines under isocratic conditions (water/acetonitrile/TFA (90/10/0.1, v/v/v)). The retention time of the byproduct NBD-OH was only 40 s, while that for NBD-heptylamine was about 1300 s. NBD-octylamine was not eluted at a detectable level, which indicated that isocratic elution was not suitable for analyzing biological samples containing various compounds that have large differences in their polarities. For these cases, a gradient elution was necessary. Figure 6-8 (b) and (c) show that aliphatic NBD amines were separated under gradient elution with gradient times of 450 s and 90 s. The analysis times for aliphatic NBD amines under gradient elution were greatly shortened compared with those under isocratic elution. It was also concluded that the retention time became shorter with the shortening of gradient time. When the gradient times were 90 s, the NBD amines could be separated within 110 s. For NBD-heptylamine, the retention time under gradient elution was one-tenth less

than that under the isocratic condition. These results show that the integration of a gradient elution system with pillar array columns is useful for quickly analyzing complex samples.

6.4 Conclusions

A gradient elution system for pressure-driven LC and pillar array columns was successfully integrated on a 20 × 20 mm silicon chip. A cross-Tesla mixer, which was utilized in the gradient system, mixed two liquids efficiently. Under the gradient elution condition, two coumarin dyes were separated within a time shorter than that under the isocratic elution condition. The peak widths of the two dyes were smaller under the gradient elution condition. Using the proposed gradient elution method, the separation efficiency of the pillar array columns was improved, as evidenced by the gradient chromatographic separation of the fluorescent derivatives of four aliphatic amines within 110 s. This elution system could potentially be employed as a tool to analyze complex biological samples.

Figures

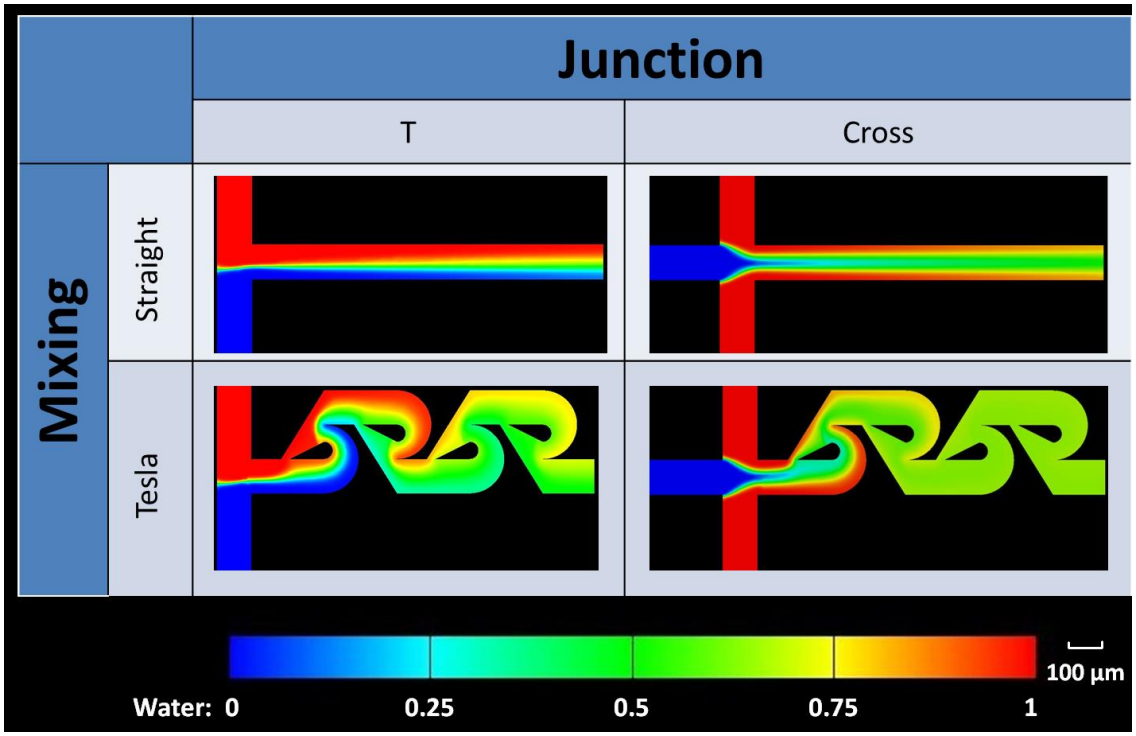

Figure 6-1. Simulation results determined by CFD analysis of the mixing of water and ethanol in the T–straight mixer, the cross-straight mixer, the T-Tesla mixer, and the cross-Tesla mixer

(a)

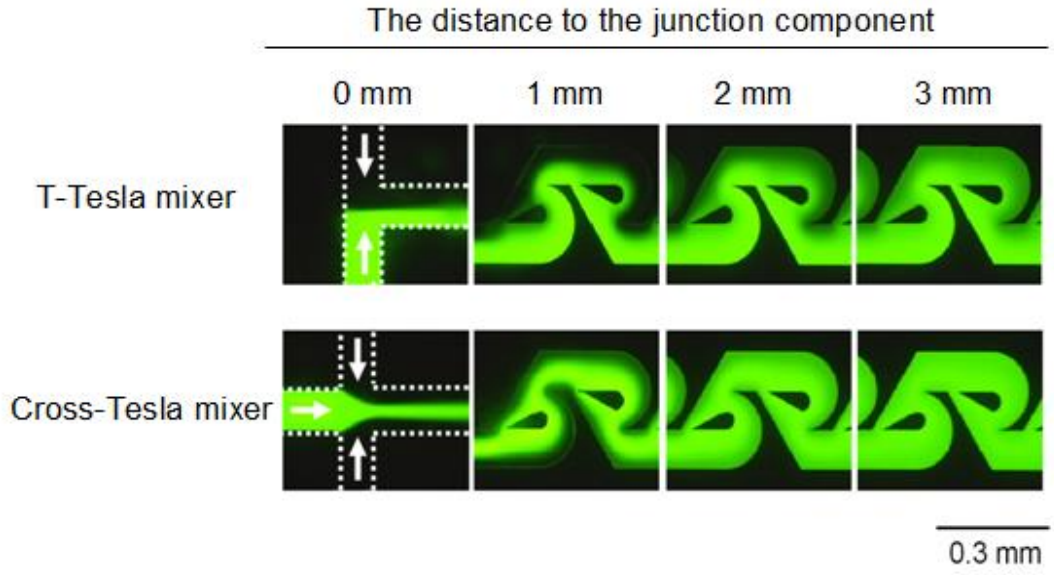

(b)

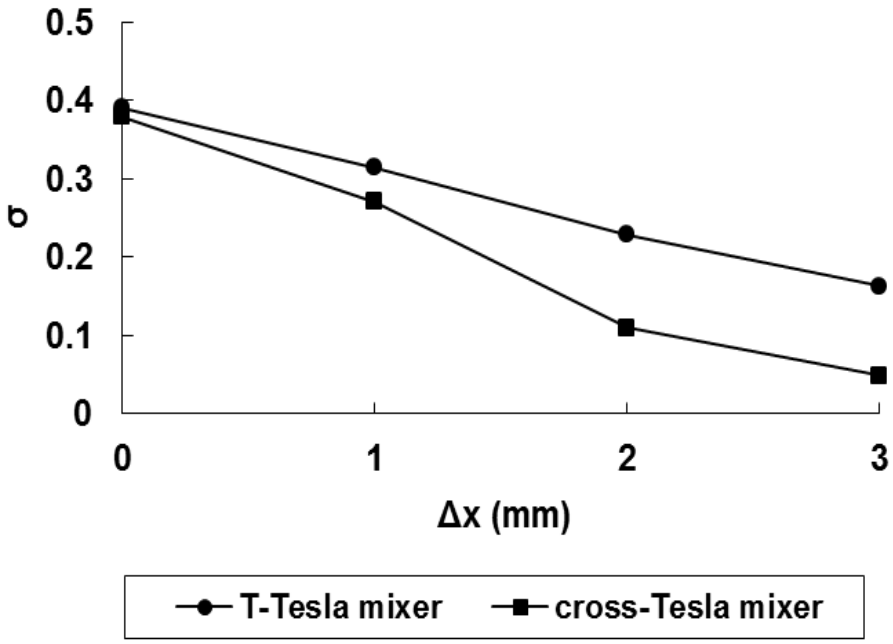

Figure 6-2. (a) Fluorescent images of the mixing of two liquids (water and fluorescein in methanol) at various positions in the two micromixers: T-Tesla mixer and cross-Tesla mixer. (b) Standard deviation of the fluorescence intensity in images of (a) as a function of the downstream position.

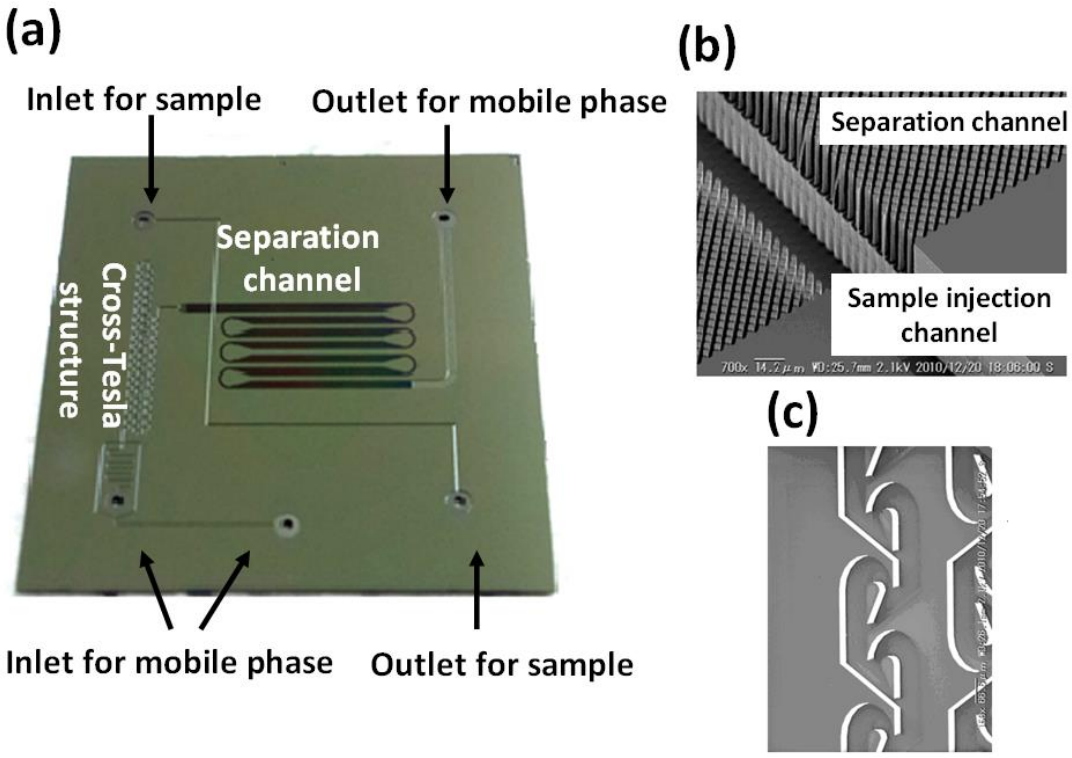

Figure 6-3. (a) A photograph of the fabricated microchip, (b) magnified view of the pillar array column and sample injection channel, and (c) magnified view of the cross-Tesla mixer

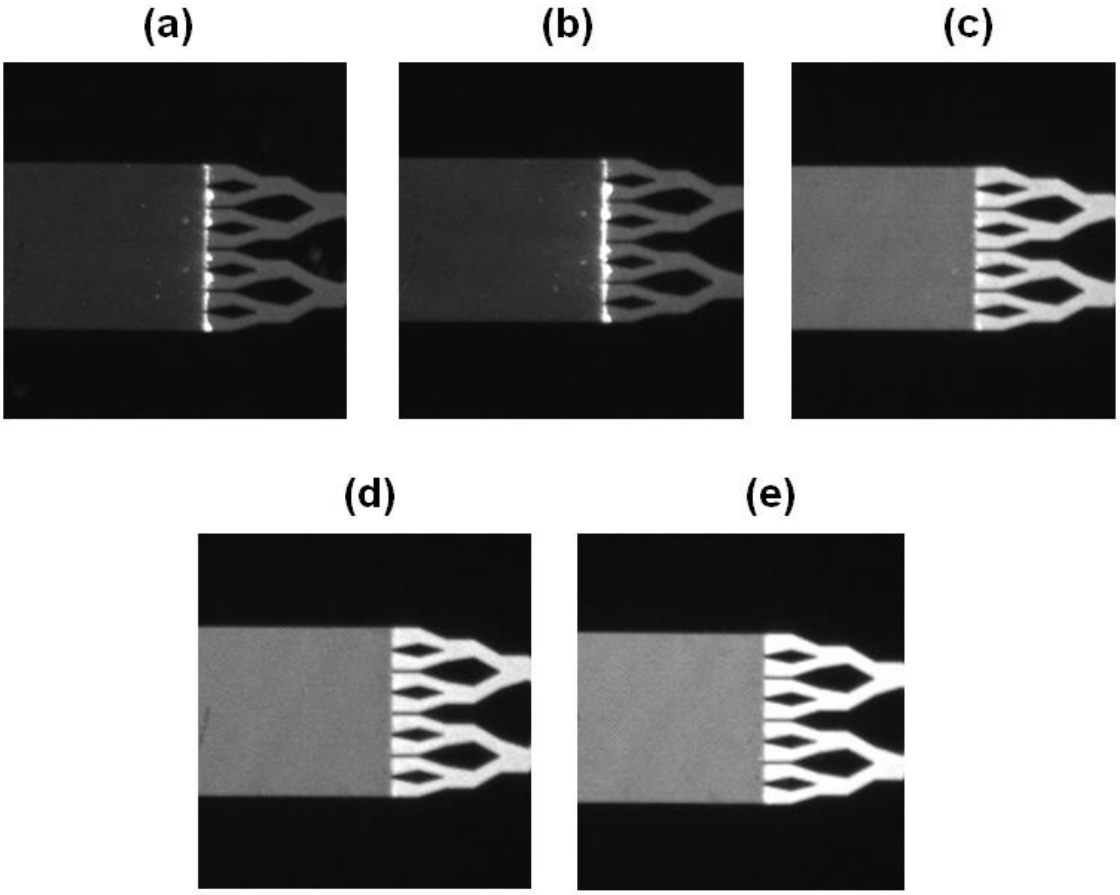

Figure 6-4. Fluorescence images of the entrance of separation channel. The two kinds of mobile phases were eluted isocratically at the total flow rate of 1 μL/min. The ratios of water and fluorescein in methanol were (a) 9:1, (b) 7:3, (c) 5:5, (d) 3:7, and (e) 1:9, respectively.

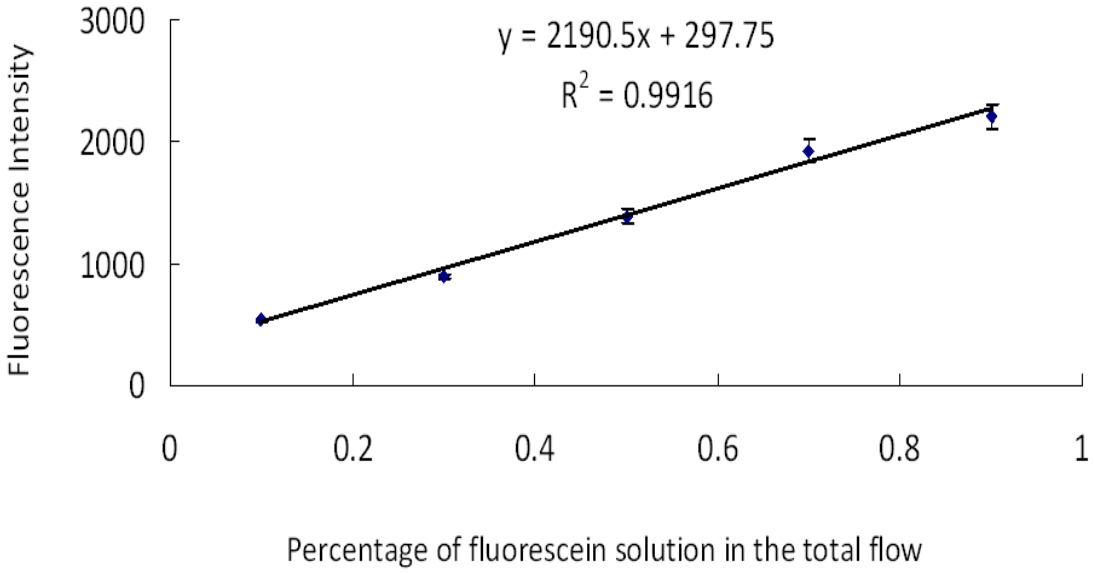

Figure 6-5. Relationship between percentage of fluorescein solution in the total flow and fluorescence intensity

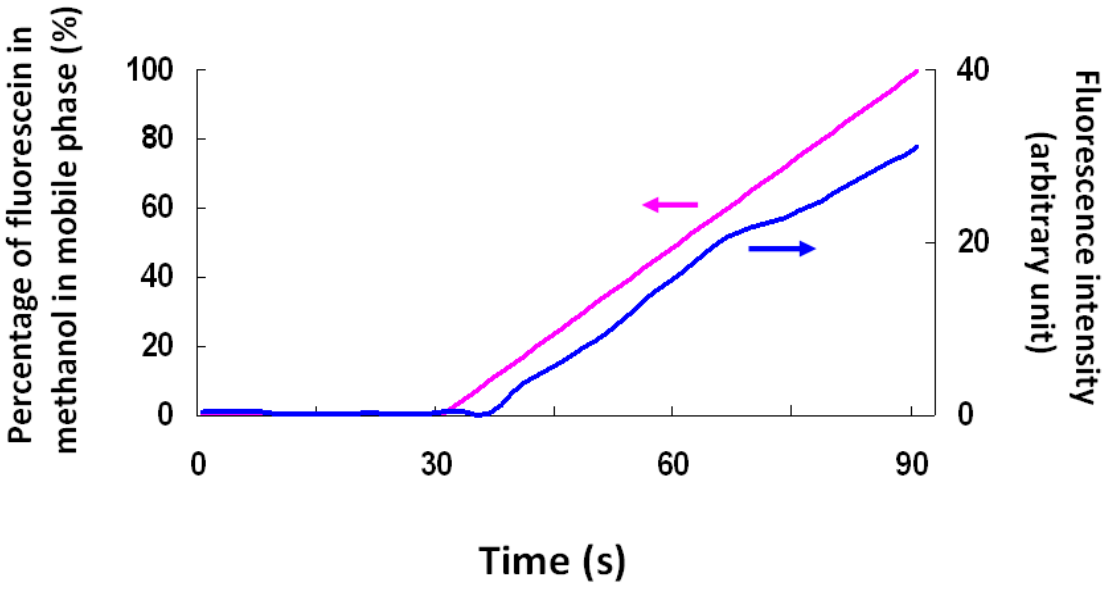

Figure 6-6. Relationship between the fluorescence intensity and analysis time

The red line stands for the change of percentage of fluorescein in methanol in mobile phase, and the blue line is the change of fluorescence intensity

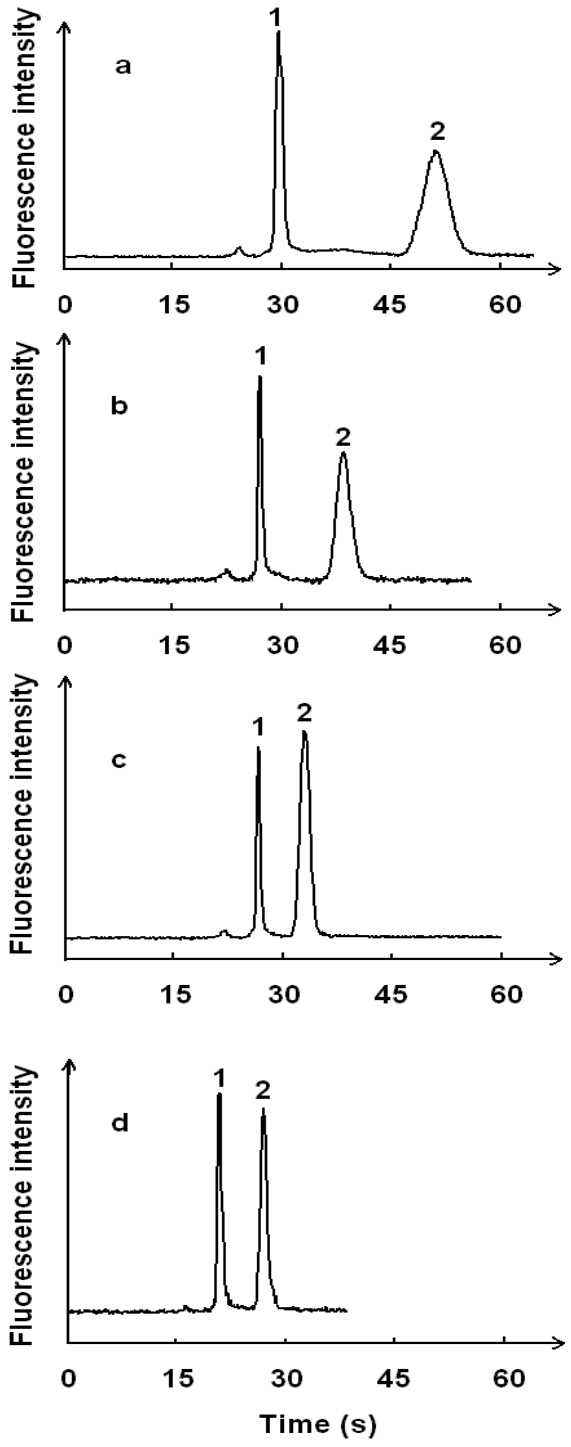

Figure 6-7. Chromatograms of the separation of Coumarin 525 (peak 1) and Coumarin 545 (peak 2) obtained under the isocratic elution condition (a), mobile phase: water/acetonitrile (65/35) and gradient elution, mobile phase: water/acetonitrile (0 s, 65/35; end, 0/100); gradient time: (b) 120 s, (c) 60 s, and (d) 30 s.

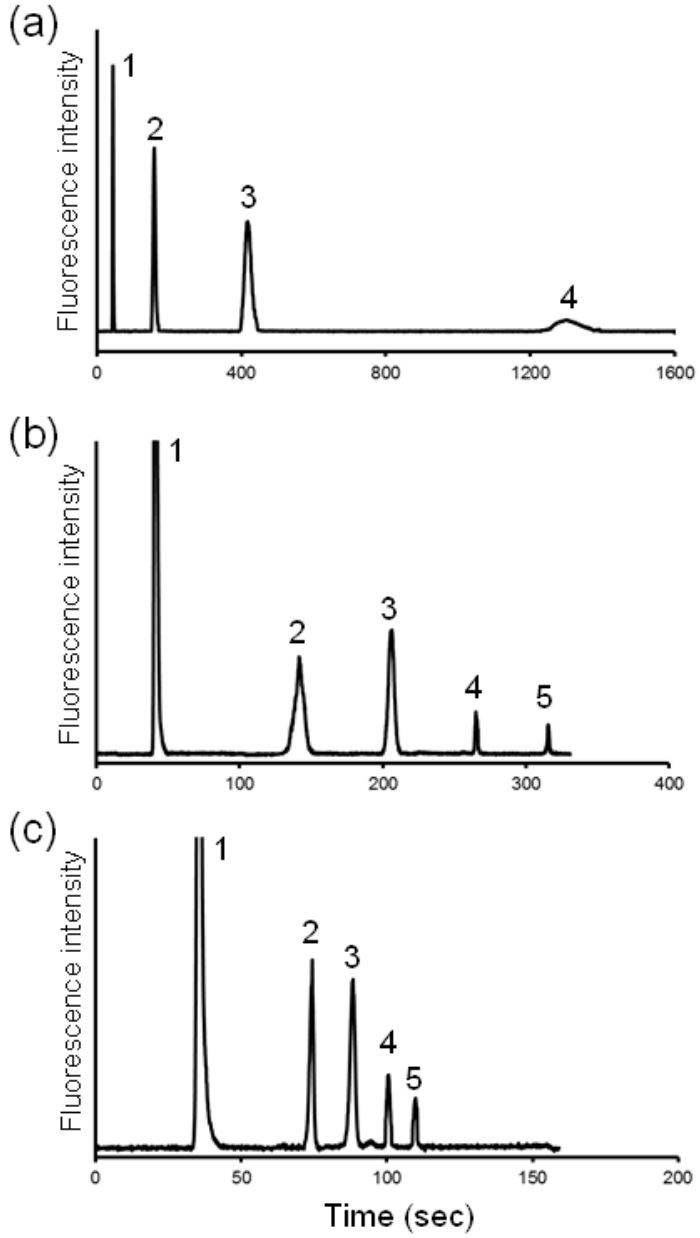

Figure 6-8. Chromatograms of separation of NBD-amines obtained under isocratic elution (a), mobile phase: water/acetonitrile/TFA (90/10/0.1) and gradient elution, mobile phase A: water/acetonitrile/TFA (90/10/0.1), mobile phase B: water/acetonitrile/TFA (10/90/0.1), gradient program (0 s, 100/0; end, 0/100); gradient time: (b), 450 s; and (c), 90 s. Peaks: 1, NBD-OH; 2, NBD-pentylamine; 3, NBD-hexylamine; 4, NBD-heptylamine; 5, NBD-octylamine.

Tables

Table 6-1. Peak widths for Coumarin 525 and 545 under isocratic and gradient elution conditions

Peak width (s)	Isocratic elution	Gradient elution		
		120 s	60 s	30 s
Coumarin 525	2.2	1.7	1.5	1.4
Coumarin 545	6.9	5.1	3.0	2.1

Chapter 7. Conclusions

7.1 Summary

In this study, two types of newly developed column, monolithic silica column and core-shell particle column were respectively utilized for the analysis of amino acids, which were involved in many biological activities. The analysis of 21 NBD-amino acids could be achieved in 7 min, which was much faster comparing with previous studies. These methods were successfully applied for the analysis of biological samples, and proved to be accurate and applicable. The developed methods can be used for routine analyses using conventional instruments in common laboratories, however, these methods still could not meet the demand for fast and quantitative analysis of biological samples in clinical field.

Therefore, pillar array column, which can great improve the separation efficiency comparing with best packed column, were utilized in the following research. To date, pillar array column have not been used for quantitative analysis. In order to verify that pillar array column could be applied for quantitative analysis of compounds in biological samples, BCAAs were selected and analyzed. The analysis of fluorescently labeled BCAAs was achieved in 100 s. By adding an internal standard, the concentrations of BCAAs in sports drink and human plasma samples were quantitatively determined. The concentrations determined using the developed method were similar with data obtained using conventional LC, which indicated that the method is applicable for analysis of biological samples.

In order to apply the pillar array column for the analysis of complex compounds in biological samples, a gradient elution system with a cross-Tesla mixer for the effective mixing of two solutions was integrated with pillar array column on a 20 × 20 mm microchip. The separation of two dyes under gradient elution was successfully

performed within half the time needed for isocratic elution. The peak widths of the two dyes were smaller under the gradient elution condition. Using the proposed gradient elution condition, the analysis time of the fluorescent derivatives of four aliphatic amines was approximately 110 s. This elution system could be employed as a promising tool to analyze complex biological samples.

7.2 Future work

The fast and quantitative analysis of compounds in biological samples has been developed by pillar array column. However, several issues should be considered in the near future.

Firstly, a precise sample injection is very essential for an analytical system, however, in our chip-LC system, injection amount is too small to be controlled. In this case, another injection mode, such as air-controlled pressure-driven injection or droplet-based injection may be available for solving this problem.

Secondly, in our chip-LC system, fluorescence microscopy was used for a more sensitive detection. However, most molecules are not intrinsically fluorescent and thus must be labeled with a fluorescent tag prior to analysis. Conventionally, this labeling reaction was performed off the chip, and in many cases takes a long time and large consumption of reagents. Therefore, developing a sample derivatization on a chip will be time-saving and make the performance easily.

Thirdly, there are many essential compounds with trace amounts in the biological samples, however, it is very difficult to conduct precise analysis of trace compounds without interference from other compounds. In order to solve this problem, solid phase extraction, which functions for sample clean-up and preconcentration, is helpful for analysis the trace compounds in biological samples. Therefore, the integration of solid phase extraction and pillar array column on a microchip should be considered.

Besides, with regard to the application, the developed method has not been used

in the clinical field. The developed fast and quantitative analysis of biological samples will be useful for the research of disease mechanism and disease diagnosis in the following work.

References

[1] L. Zhu, A. Bhattacharyya, E. Kurali, A. Anderson, A. Menius, K. Lee, Statistics in Biopharmaceutical Research, 3 (2011) 561-568.

[2] Y. Ma, P. Zhang, Y. Yang, F. Wang, H. Qin, Molecular Biology Reports, 39 (2012) 7505-7511.

[3] A. Zhang, H. Sun, X. Wang, Analytical and Bioanalytical Chemistry, 404 (2012) 1239-1245.

[4] P. Masson, A.C. Alves, T.M.D. Ebbels, J.K. Nicholson, E.J. Want, Analytical Chemistry, 82 (2010) 7779-7786.

[5] S. Rochfort, Journal of Natural Products, 68 (2005) 1813-1820.

[6] D. Ryan, K. Robards, Analytical Chemistry, 78 (2006) 7954-7958.

[7] W. Weckwerth, Metabolomics: methods and protocols, Humana Press, (2007).

[8] M.K.R. Mudiam, C. Ratnasekhar, R. Jain, P.N. Saxena, A. Chauhan, R.C. Murthy, Journal of Chromatography B-Analytical Technologies in the Biomedical and Life Sciences, 907 (2012) 56-64.

[9] M. Saraji, N. Mehrafza, A.A.H. Bidgoli, M.T. Jafari, Journal of Separation Science, 35 (2012) 2637-2644.

[10] D. Tsikas, C.E. Evans, T.T. Denton, A. Mitschke, F.-M. Gutzki, J.T. Pinto, T. Khomenko, S. Szabo, A.J.L. Cooper, Analytical Biochemistry, 430 (2012) 4-15.

[11] E. Ban, E.J. Song, Journal of Chromatography B-Analytical Technologies in the Biomedical and Life Sciences, 929 (2013) 180-186.

[12] C. Barbas, E.P. Moraes, A. Villasenor, Journal of Pharmaceutical and Biomedical Analysis, 55 (2011) 823-831.

[13] L. Liu, F. Feng, S. Shuang, Y. Bai, M.M.F. Choi, Talanta, 91 (2012) 83-87.

[14] L. Adlnasab, H. Ebrahimzadeh, Y. Yamini, F. Mirzajani, Talanta, 83 (2010) 370-378.

[15] L. He, K. Zhang, C. Wang, X. Luo, S. Zhang, Journal of Chromatography A, 1218 (2011) 3595-3600.

[16] H. Xu, S. Wang, G. Zhang, S. Huang, D. Song, Y. Zhou, G. Long, Analytica Chimica Acta, 690 (2011) 86-93.

[17] A.J.P. Martin, R.L.M. Synge, Biochemical Journal, 35 (1941) 1358-1368.

[18] F. Gritti, G. Guiochon, Analytical Chemistry, 85 (2013) 3017-3035.

[19] J. Eijkel, Lab on a Chip, 7 (2007) 815-817.

[20] P.W. Carr, D.R. Stoll, X. Wang, Analytical Chemistry, 83 (2011) 1890-1900.

[21] K.K. Unger, R. Skudas, M.M. Schulte, Journal of Chromatography A, 1184 (2008) 393-415.

[22] S. Fekete, K. Ganzler, J. Fekete, Journal of Pharmaceutical and Biomedical Analysis, 54 (2011) 482-490.

[23] F. Gritti, J. Omamogho, G. Guiochon, Journal of Chromatography A, 1218 (2011) 7078-7093.

[24] J.H. Knox, Journal of Chromatography A, 831 (1999) 3-15.

[25] J.H. Knox, Journal of Chromatography A, 960 (2002) 7-18.

[26] B. He, F. Regnier, Journal of Pharmaceutical and Biomedical Analysis, 17 (1998) 925-932.

[27] B. He, N. Tait, F. Regnier, Analytical Chemistry, 70 (1998) 3790-3797.

[28] N.V. Lavrik, L.T. Taylor, M.J. Sepaniak, Analytica Chimica Acta, 694 (2011) 6-20.

[29] W. De Malsche, H. Eghbali, D. Clicq, J. Vangelooven, H. Gardeniers, G. Desmet, Analytical Chemistry, 79 (2007) 5915-5926.

[30] W. De Malsche, J.O. De Beeck, S. De Bruyne, H. Gardeniers, G. Desmet, Analytical Chemistry, 84 (2012) 1214-1219.

[31] W. De Malsche, S. De Bruyne, J.O. De Beek, P. Sandra, H. Gardeniers, G. Desmet, F. Lynen, Journal of Chromatography A, 1230 (2012) 41-47.

[32] C. Aoyama, A. Saeki, M. Noguchi, Y. Shirasaki, S. Shoji, T. Funatsu, J. Mizuno, M. Tsunoda, Analytical Chemistry, 82 (2010) 1420-1426.

[33] G. Wu, Amino Acids, 37 (2009) 1-17.

[34] T. Hisamatsu, S. Okamoto, M. Hashimoto, T. Muramatsu, A. Andou, M. Uo, M.T. Kitazume, K. Matsuoka, T. Yajima, N. Inoue, T. Kanai, H. Ogata, Y. Iwao, M.

Yamakado, R. Sakai, N. Ono, T. Ando, M. Suzuki, T. Hibi, Plos One, 7 (2012) e31131.

[35] T.J. Wang, M.G. Larson, R.S. Vasan, S. Cheng, E.P. Rhee, E. McCabe, G.D. Lewis, C.S. Fox, P.F. Jacques, C. Fernandez, C.J. O'Donnell, S.A. Carr, V.K. Mootha, J.C. Florez, A. Souza, O. Melander, C.B. Clish, R.E. Gerszten, Nature Medicine, 17 (2011) 448-453.

[36] F. Mochel, S. Benaich, D. Rabier, A. Durr, Archives of Neurology, 68 (2011) 265-267.

[37] P.-F. Gao, Z.-X. Zhang, X.-F. Guo, H. Wang, H.-S. Zhang, Talanta, 84 (2011) 1093-1098.

[38] M.T. Kelly, A. Blaise, M. Larroque, Journal of Chromatography A, 1217 (2010) 7385-7392.

[39] B. Redruello, V. Ladero, I. Cuesta, J.R. Alvarez-Buylla, M. Cruz Martin, M. Fernandez, M.A. Alvarez, Food Chemistry, 139 (2013) 1029-1035.

[40] M. Krizman, I. Virant-Klun, M. Prosek, Journal of Chromatography B-Analytical Technologies in the Biomedical and Life Sciences, 858 (2007) 292-295.

[41] T. Mohabbat, B. Drew, Journal of Chromatography B-Analytical Technologies in the Biomedical and Life Sciences, 862 (2008) 86-92.

[42] S.A. Cohen, D.P. Michaud, Analytical Biochemistry, 211 (1993) 279-287.

[43] A. Jambor, I. Molnar-Perl, Journal of Chromatography A, 1216 (2009) 3064-3077.

[44] V. Pereira, M. Pontes, J.S. Camara, J.C. Marques, Journal of Chromatography A, 1189 (2008) 435-443.

[45] S.L. Grant, Y. Shulman, P. Tibbo, D.R. Hampson, G.B. Baker, Journal of Chromatography B-Analytical Technologies in the Biomedical and Life Sciences, 844 (2006) 278-282.

[46] C. Aoyama, T. Santa, M. Tsunoda, T. Fukushima, C. Kitada, K. Imai, Biomedical Chromatography, 18 (2004) 630-636.

[47] S. Nonaka, M. Tsunoda, C. Aoyama, T. Funatsu, Journal of Chromatography B-Analytical Technologies in the Biomedical and Life Sciences, 843 (2006) 170-174.

[48] S. Nonaka, M. Tsunoda, K. Imai, T. Funatsu, Journal of Chromatography A, 1066 (2005) 41-45.

[49] M. Tsunoda, S. Nonaka, T. Funatsu, Analyst, 130 (2005) 1410-1413.

[50] C. Aoyama, M. Tsunoda, T. Funatsu, Analytical Sciences, 25 (2009) 63-65.

[51] G.L. Li, Z.W. Sun, C.H. Song, L. Xia, J. Zheng, Y.R. Suo, J.M. You, Biomedical Chromatography, 25 (2011) 689-696.

[52] L. Wang, R.J. Xu, B. Hu, W. Li, Y. Sun, Y.Y. Tu, X.X. Zeng, Food Chemistry, 123 (2010) 1259-1266.

[53] R. Rebane, K. Herodes, Analytica Chimica Acta, 672 (2010) 79-84.

[54] W.A.H. Waterval, J.L.J.M. Scheijen, M.M.J.C. Ortmans-Ploemen, C.D.H.-v.d. Poel, J. Bierau, Clinica Chimica Acta, 407 (2009) 36-42.

[55] X. Hu, C.W. Bolten, Drug Development Research, 67 (2006) 871-883.

[56] M.M. Fung, O.H. Viveros, D.T. O'Connor, Acta Physiologica, 192 (2008) 325-335.

[57] H.N. Munro, M.H. Steele, Hutchiso.Wc, British Journal of Nutrition, 19 (1965) 137-147.

[58] M. Tsunoda, K. Imai, Analytical and Bioanalytical Chemistry, 380 (2004) 887-890.

[59] M.L. Jirout, R.S. Friese, N.R. Mahapatra, M. Mahata, L. Taupenot, S.K. Mahata, V. Kren, V. Zidek, J. Fischer, H. Maatz, M.G. Ziegler, M. Pravenec, N. Hubner, T.J. Aitman, N.J. Schork, D.T. O'Connor, Human Molecular Genetics, 19 (2010) 2567-2580.

[60] R.A.K. Rao, M. Ajmal, B.A. Siddiqui, S. Ahmad, Environmental Monitoring and Assessment, 54 (1999) 289-299.

[61] C.T. Mant, R.S. Hodges, Journal of Chromatography A, 972 (2002) 45-60.

[62] Y. Song, T. Funatsu, M. Tsunoda, Journal of Chromatography B-Analytical Technologies in the Biomedical and Life Sciences, 879 (2011) 335-340.

[63] Q. Gu, X. Shi, P. Yin, P. Gao, X. Lu, G. Xu, Analytica Chimica Acta, 609 (2008) 192-200.

[64] Y. Song, T. Funatsu, M. Tsunoda, Amino Acids, 42 (2012) 1897-1902.

[65] J.T. Brosnan, Journal of Nutrition, 133 (2003) 2068S-2072S.

[66] F. Yoshizawa, Biochemical and Biophysical Research Communications, 313 (2004) 417-422.

[67] L.K. Bak, M.L. Johansen, A. Schousboe, H.S. Waagepetersen, Journal of Neuroscience Research, 90 (2012) 1768-1775.

[68] Rosentha.J, A. Angel, J. Farkas, American Journal of Physiology, 226 (1974) 411-418.

[69] S.H. Korman, Molecular Genetics and Metabolism, 89 (2006) 289-299.

[70] M.G. Gioia, P. Andreatta, S. Boschetti, R. Gatti, Journal of Pharmaceutical and Biomedical Analysis, 45 (2007) 456-464.

[71] R. Kand'ar, P. Zakova, J. Jirosova, M. Sladka, Clinical Chemistry and Laboratory Medicine, 47 (2009) 565-572.

[72] N. Kiba, Y. Oyama, A. Kato, M. Furusawa, Journal of Chromatography A, 724 (1996) 354-357.

[73] J. Sowell, L. Pollard, T. Wood, Journal of Separation Science, 34 (2011) 631-639.

[74] K. Uchikura, Chemical & Pharmaceutical Bulletin, 51 (2003) 1092-1094.

[75] Y. Song, T. Funatsu, M. Tsunoda, Journal of Chromatography B-Analytical Technologies in the Biomedical and Life Sciences, 927 (2013) 214-217.

[76] W. De Malsche, S. De Bruyne, J.O. De Beeck, S. Eeltink, F. Detobel, H. Gardeniers, G. Desmet, Journal of Separation Science, 35 (2012) 2010-2017.

[77] M. Tsunoda, M. Kato, T. Fukushima, T. Santa, H. Homma, H. Yanai, T. Soga, K. Imai, Biomedical Chromatography, 13 (1999) 335-339.

[78] S. Song, A.K. Singh, Analytical and Bioanalytical Chemistry, 384 (2006) 41-43.

[79] P. Calders, J.L. Pannier, D.M. Matthys, E.M. Lacroix, Medicine and Science in Sports and Exercise, 29 (1997) 1182-1186.

[80] E. Blomstrand, J. Eliasson, H.K.R. Karlsson, R. Kohnke, Journal of Nutrition, 136 (2006) 269S-273S.

[81] L.E. Norton, D.K. Layman, Journal of Nutrition, 136 (2006) 533S-537S.

[82] C.-Y. Chen, T.-Y. Tzung, C.-S. Wu, Y.-H. Chen, Dermatologica Sinica, 27 (2009) 122-127.

[83] P.d.L. Pelaez, C. Funchal, S.O. Loureiro, L. Heimfarth, A. Zamoner, C. Gottfried, A. Latini, M. Wajner, R. Pessoa-Pureur, International Journal of Developmental Neuroscience, 25 (2007) 181-189.

[84] T. Kawaguchi, N. Izumi, M.R. Charlton, M. Sata, Hepatology, 54 (2011) 1063-1070.

[85] K. Suzuki, K. Suzuki, K. Koizumi, H. Ichimura, S. Oka, H. Takada, H. Kuwayama, Hepatology Research, 38 (2008) 267-272.

[86] Y. Huang, M. Zhou, H. Sun, Y. Wang, Cardiovascular Research, 90 (2011) 220-223.

[87] T. Kutsuzawa, S. Shioya, D. Kurita, M. Haida, Clinical Nutrition, 28 (2009) 203-208.

[88] L.M. Belalcazar, C.M. Ballantyne, Current Opinion in Lipidology, 22 (2011) 503-504.

[89] T. Kuzuya, Y. Katano, I. Nakano, Y. Hirooka, A. Itoh, M. Ishigami, K. Hayashi, T. Honda, H. Goto, Y. Fujita, R. Shikano, Y. Muramatsu, G. Bajotto, T. Tamura, N. Tamura, Y. Shimomura, Biochemical and Biophysical Research Communications, 373 (2008) 94-98.

[90] P. Felig, E. Marliss, G.F. Cahill, New England Journal of Medicine, 281 (1969) 811-816.

[91] E. Mery, F. Ricoul, N. Sarrut, O. Constantin, G. Delapierre, J. Garin, F. Vinet, Sensors and Actuators B: Chemical, 134 (2008) 438-446.

[92] V. Hessel, H. Lowe, F. Schonfeld, Chemical Engineering Science, 60 (2005) 2479-2501.

[93] M. Kakuta, F.G. Bessoth, A. Manz, The Chemical Record, 1 (2001) 395-405.

[94] A.D. Stroock, S.K.W. Dertinger, A. Ajdari, I. Mezic, H.A. Stone, G.M. Whitesides, Science, 295 (2002) 647-651.

[95] N.T. Nguyen, Z.G. Wu, Journal of Micromechanics and Microengineering, 15 (2005) R1-R16.

[96] J.X. Li, M.Y. Zhang, L.M. Wang, W.H. Li, P. Sheng, W.J. Wen, Microfluidics and Nanofluidics, 10 (2011) 919-925.

[97] S.S. Wang, Z.J. Jiao, X.Y. Huang, C. Yang, N.T. Nguyen, Microfluidics and Nanofluidics, 6 (2009) 847-852.

[98] C.C. Hong, J.W. Choi, C.H. Ahn, Lab on a Chip, 4 (2004) 109-113.

[99] A. Asgar, S. Bhagat, I. Papautsky, Journal of Micromechanics and Microengineering, 18 (2008) 085005.

Acknowledgements

I would like to express my sincere gratitude and deep appreciation to my supervisor Professor Takashi FUNATSU and Lecturer Makoto TSUNODA, for their valuable supervisions and supports. They gave me so many kind helps during my four years' life in Japan.

I would like to thank Professor Shuichi SHOJI (Major in Nano-Science and Nano-Engineering, Waseda University, Japan) for his valuable suggestions that contributed to my thesis.

I want to thank Chiaki AOYAMA (GL sciences Inc. Japan), Masao NOGUCHI and Katsuya TAKATSUKI (Major in Nano-Science and Nano-Engineering, Waseda University, Japan) for their help during my research.

My special thanks go to Japanese Government (MEXT) Scholarship for supporting me from Oct. 2009 to Sep. 2013.

Also, many thanks go to all the members of FUNATSU Laboratory, Lecture Kikuchi and staff of International Student Advising Room, and my Japanese teachers Sumiyo INAMURA and Masayoshi NAKAMURA who helped me a lot during my study and life.

I also want to thank my parents and friends for always supporting me.

2013.08

宋　彦廷
Yanting SONG